npg-2020-4 : Anthropocene climate bifurcation AUTHORS' RESPONSE

Kolja Leon Kypke, William Finlay Langford, and Allan Richard Willms

Department of Mathematics and Statistics, University of Guelph, 50 Stone Road West, Guelph, ON, Canada N1G 2W1

Correspondence: William F. Langford (wlangfor@uoguelph.ca)

1 Comments from referees

1.1 Referee 1 comments

Peter Ditlevsen (Referee) pditlev@nbi.ku.dk
Received and published: 10 March 2020.
In this paper an energy balance model (EBM), presented in (Dortmans, 2019), containing a surface (represented by a surface temperature) and a single layer atmosphere (represented by the atmospheric radiation) is forced with increasing greenhouse gas concentrations following the four IPCC RCP scenarios. The EBM can represent different zonal bands, or the polar regions with oceanic and atmospheric heat fluxes across the zonal boundary. The model includes ice albedo and water vapor feedbacks and an implicit ocean and atmosphere heat transport feedback.

The model has a bimodal regime with a saddle node bifurcation to a warm polar region state, which will be reached after the next century if the CO_2 level reaches 2000 ppm. The mechanism responsible for the bifurcation structure is via the sigmoidal dependence of ice albedo on temperature, essentially similar to Budyko-Sellers EBM. In the parameter space spanned by the atmospheric CO_2 concentration, the water vapor relative humidity, the oceanic heat transport and the steepness of the albedo switch, there is a cusp separating the fold and a mono-stable state. The paper is well written, and I recommend publication. The authors might, however, consider a few revisions, which in my view would make it even more readable:

First of all, it is always a delicate balance, how much material to repeat from previous papers, in this case the reference above introducing the model. In my view it is either or: Either the reader is required to also consult other papers, or the paper should be fully self-contained. In the latter case a few additions would be helpful:

Explain the asymmetry between eqs. 1 and 2: Why use I_A and not T_A as variable? As is now, both have dimensions of Wm^{-2}, with the consequence of different dimensionalities for c_S and c_A. This confused me at first.

Eq 10 for vertical heat transport f_C seems overly complicated for such a simple EBM. It is stated that the formula is obtained (derived, I take it) in (Kypke 2019). This a PhD thesis, which is not easily accessible for the reader. Consider at least hinting at where it comes from. Perhaps even a graph, f_C as a function of T_S. Though hard to read, I think there is a ")" missing (same goes for eq 22).

Now the mathematical analysis begins with Eqs 15 and 16: It would be helpful to remind the reader that μ enters via η (through eq. 9), since μ will be the "control parameter" in the following.

A few more remarks:

Figure 6 (a) shows the responses in the four cases before the bifurcation point. These responses are quite linearly related to the RCPs (Figure 4). The same goes for the GCM scenarios presented in IPCC AR5 (Fig AI.8). The statement (line 239) that the EBM results are in good agreement with the GCM projections is thus an overstatement, both are related to the RCPs.

The bifurcation for the Arctic and not the global EBM depends critically on the oceanic heat transport F_O. It would be useful with a comparison of this EBM with the classical 1-d EBMs where meridional heat transport is modelled as a diffusion.

1.2 Referee 2 comments

Michel Crucifix (Referee) michel.crucifix@uclouvain.be
Received and published: 4 May 2020
This article provides an improvement on the classical energy balance model (EBM) provided by the prognostic equations (1) and (2). These prognostic equations are the same as those

nowadays found in textbooks, and based on the pioneering works of Budyko and Sellers. It is applied at a regional scale, hence a F_O term accounts for the net supply of heat by ocean transport. Compared to the textbook formulations, the diagnostic equations are more elaborate. These are equation (6) to (10), and include specific parametrisations for sensible and latent heat transport, with details given in the lead author master?s thesis. The albedo feedback given by equation (8) follows the fairly standard hyperbolic tangent formulation, and it is here presented as a consequence of the dynamics of sea ice.

Expectedly, the model presents bifurcations caused by the albedo dependence on temperature, as already studied by Budyko and Sellers, North, Ghil, and others. The claim of the authors is that the diagnostic equations have been given more attention in the present contribution, and are more accurate than in previous works, such that their model can be used for actual predictions of climate in the 21st century and beyond (most plots extend to 2300). Specifically, the authors present previous EBMs as "lacking in the geophysical details and mathematical rigour required to make useful predictions". They go on: "This paper presents an EBM built upon basic laws of geophysics" and "it provides new mathematical evidence signifying that catastrophic climate change in polar regions is inevitable in the coming decades and centuries if current anthropogenic forcing continues unabated". This conclusion follows from a bifurcation analysis of the model, and the identification of co-dimension 2 (cusp) bifurcations in the parameter space spanned by the CO_2 concentration and the net heat flux penetrating the domain studied.

Overall, I support the publication of this contribution. However, I believe that the positioning of this study with respect to the state-of-the-art is arguable. On the one hand, the claim that earlier studies have been "lacking mathematical rigour" seems somewhat excessive (the recent review of Ghil and Lucarini, 2019, arXiv 1910.00583, is a nice entry point, which shows how much mathematics has already gone in previous works). I would also not say that they did not provide "useful" predictions. On the other hand, they present general circulation models (GCM) as "too stable" to provide reliable warning on the sudden catastrophic events, citing Valdes (2011). Indeed, low-dimensional models tend to have a more clear-cut bifurcation structure than high-dimensional models such as GCMs, but there are also good reasons for the smoother character of certain transitions in the GCMs (spatial patterns, partial capture of scaling laws, effects of turbulence). In particular, a number of simulations with so-called earth models of intermediate complexity have been run well into the future and they do not necessarily present such "catastrophic" transitions; it would be legitimate to ask why they didn't so, while they certainly include more "geophysical detail" than the current study. The interest of an EBM bifurcation analysis is not so much to provide an accurate prediction that would supersede the current state-of-the-art. It rather lies in sensitivity analysis and examination of the conditions that would generate a bifurcation (see, in particular, my comments below regarding line 109). I would also like to make a few comments about the semantics.

There is an important distinction to be made between the existence of a bifurcation, and the potentially abrupt character of a transition (l. 50). The bifurcation, at least the way it is presented here, tells us about the topology of the attractor, which is a measure of the invariant manifold. The "abruptness" relates to the dynamics of the transient changes that occur when the system moves from one fixed point to the other. The existence of a bifurcation does not imply abruptness. Think of the melting of large ice sheets (incidentally, lacking in the present model). One way to address this ambiguity is to consider the dynamics of non-autonomous systems, as done for example with "mathematical rigour" by Ashwin et al. (2012, doi: 10.1098/rsta.2011.0306). Furthermore, I would advise caution with the arguments that using "basic laws of geophysics" generates more accuracy (ll. 30-35). No climate model is computed "ab initio". Any model requires parametrizations which always include an empirical component, and the very simple EBM presented here is certainly no exception. Furthermore, the dynamics of climate are also related to biology and therefore involves knowledge and arguments that go beyond geophysics. With these reservations expressed, I would like to reiterate that I am overall supportive to the publication of this paper, and we now proceed with the line-by-line comments.

1. l. 109 - The difference between α_c and α_w is quite large, and it seems pretty clear that the bifurcation depends on the amplitude of this difference, and on the slope of $\alpha(T)$ curve (as can be seen with a Lamerey diagram, in the way done by, e.g., Brovkin et al., 10.1029/1998JD200006). In the real world, the spatial distribution and seasonal cycles of snow and ice are likely to effectively smooth the albedo dependency expressed by equation (8).
2. l. 174 - β_1 and β_2: aren't these ζ_1 and ζ_2 ?
3. l. 176 - Start with a section 3.1.
4. l. 210 - Given that the definition of albedo function is so important for the existence (and significance) of bifurcations, it is necessary to be very explicit about the latitudes covered.
5. Figure 6 - Again, the arrow sketched on figure b should not be interpreted as if the transition was instantaneous. More generally, what are drawn here are steady states, while actual trajectories depart from the steady state.
6. Section 3.2.2 - Whether the heat flux will increase with global warming is arguable. For example, if Greenland melts, the thermohaline circulation may reduce in intensity, and so would the supply of heat to the high latitudes. If sea ice melts, the thermal contrast between the Atlantic and Arctic will also change, and the consequences on ocean and atmospheric transport are not necessarily trivial.
7. l. 304 - "the EBM predicts that CO_2 mitigation strategies, if introduced soon enough, may avert the drastic consequences of this bifurcation." We have to be careful about writing such sentences. This paper is not about mitigation

strategies. We are not discussing what would be the effect of policies on CO2 emissions and CO2 concentrations. So the EBM predicts nothing about mitigation strategies. It only predicts that conservative RCP scenarios avoid the bifurcation.

8. l. 319 - It might be good to write somewhere explicitly that land ice masses are considered as constant in this study (I might have missed this, though)

9. l. 382 : the IPCC is "reporting" (results of published work), not "predicting".

10. l. 398 - It is correct that for 4.55° C is a reasonable number, though on the high range, but the last part of the argument seems a little bit overstretched. Some GCMs have a low climate sensitivity, too, and yet they rely on what the authors call "geophysics".

11. l. 400 : "based on geophysics rather than statistical data": I would write "based on physical rather than statistical modelling" (though, to be fair, several assumptions included in the physical model are based on statistical modelling or regressions, but we understand what is being said here).

12. l. 409 - "the analysis of this paper presents a mathematical proof that a bifurcation can occur in an EBM": this is correct but again I would do justice to other authors who already presented bifurcation analysis in EBMs.

13. l.423 - The author nicely present their plans for the next years with the project to develop a 3D model. What is the intended added value compared to existing initiatives like PLASIM?

14. Code availability: Especially given the stance on open source in the conclusion paragraph, I would strongly encourage the authors to provide the code necessary to reproduce the main results, either in the form of a version-controlled repository (e.g.: gitlab), or an doi-ed archive (e.g. zenodo).

2 Authors' response

2.1 Response to referee 1

The authors wish to thank Referee 1 for a careful reading of the manuscript and for insightful comments.

The referee recognizes the delicate balance between making the paper self-contained, and requiring the reader to consult earlier work. The authors will improve the readability of the manuscript, with the following clarifications and additions, as suggested by the referee.

1. The confusing asymmetry between equations (1) and (2) will be explained, and the use of I_A instead of T_A will be motivated.

2. Eq. (10) for the vertical heat transport f_C will be simplified, and its derivation will be given in the Appendix. The referee is right that there is a missing ")".

3. The crucial dependence of η on μ and δ will be clarified in eqs. (15)(16).

4. The relationship between the EBM responses shown in Fig. 6(a), and the GCM scenarios presented in IPCC AR5 Fig. AI.8 and AI.9, up to the year 2100, will be clarified. Both use the RCP scenarios to determine hypothetical CO_2 concentrations (μ) by year, out to year 2100. Then both use these CO_2 concentrations as input to the model (EBM or GCM) to determine predicted climate changes for the same period.

5. The bifurcation for the Arctic EBM depends critically on the ocean heat transport F_O. The referee suggests that it would be useful to compare this EBM with classical 1D EBMs where meridional heat transport is modelled as a diffusion. The authors' plan of future work will include determination of the meridional heat transport in more sophisticated models, and those results will be compared with this simple EBM presented here.

2.2 Response to referee 2

The authors thank Referee 2 for his constructive criticisms of the manuscript.

The referee states that this contribution needs to be better positioned with respect to the state-of-the-art. The paper appears to downplay important contributions of previous researchers. This was not intentional. The referee quotes several sentences from the Introduction to make his point. The authors will rewrite those introductory paragraphs, to better position this contribution in the discipline. The referee then correctly points out that the interest of an EBM bifurcation analysis is not to provide an accurate prediction that would supersede the current state-of-the-art. It can provide a closer examination of the conditions that would generate a bifurcation.

The referee points out that the existence of a bifurcation does not necessarily imply an abrupt transition. However, the particular bifurcations found in this manuscript combine to give the phenomenon of hysteresis, which does imply abrupt transition in a dynamical system. The authors will clarify this distinction. Also, the referee is correct in saying that the very simple EBM presented here includes an empirical component, and in fact does not rest exclusively on the basic laws of geophysics.

Line-by-line comments:

1. Yes, the difference between α_c and α_w is quite large, but these values are taken from the literature. The smoothing effect of spatial distribution and seasonal cycles have been taken into account in equation (8).

2. Yes, β_1 and β_2 should be ζ_1 and ζ_2. Thank you.

3. The authors feel that the section numbers are fine as they are.

4. The latitudes included in the Arctic model are made explicit in subsection 3.2.2. The Antarctic is similar.

5. The authors agree that the transition indicated by an arrow in Figure 6 should not be interpreted as instantaneous. In fact, just to the right of the saddlenode bifurcation point, trajectories in the phase space move upward very slowly,

through what is sometimes called the "ghost" of the saddlenode (the transit time has inverse square-root dependence on the unfolding parameter, in a small neighbourhood). Outside of that neighbourhood, trajectories have their normal velocity determined by c_S and c_A. The captions and text for Figure 6–11 will be rewritten accordingly.

6. The changes of heat flux, due to ocean and atmospheric transport, are matters of debate today. Some of this debate has been reflected in the manuscript. The melting of the Greenland ice cap surely will affect the North Atlantic – Arctic thermohaline circulation, in some way. The authors are not qualified to partake of this debate; however, this model is easily adapted to any heat flux scenario that is proposed.

7. Of course, the referee is right that this paper is not about mitigation strategies, only about the effects of various rates of CO_2 emissions. The IPCC is concerned about mitigation strategies and the effects of policy decisions. The Representative Climate Pathways (RCP) are mechanisms invented to simulate the possible effects of different mitigation strategies. This paragraph will be rewritten as suggested by the referee.

8. Correct, this study does not consider the loss of land ice masses.

9. Point taken. The IPCC is reporting, not predicting. This will be changed.

10. We are happy with our Equilibrium Climate Sensitivity (ECS) value of 4.55 C calculated for the global EBM, which is at the high end of the IPCC range. It was Priostosescu and Huybers (2017) who pointed out that statistical models tend to lie at the low end of the IPCC range, while deterministic nonlinear models like ours are at the high end. We can not explain why some GCM's have a lower climate sensitivity without examining them individually.

11. Yes, we agree, the word "geophysics" is used inappropriately here (and also in point 10). What was meant was that deterministic, nonlinear physical reasoning is at the foundation of the model, not statistical modelling.

12. The referee is right; there have been plenty of EBM's that present bifurcations, going back to Budyko, Sellers, North and others. However we have, I believe, given the first mathematical proof of the existence of a cusp bifurcation in an EBM, complete with the determination of the corresponding Center Manifold and the physical unfolding parameters. The complete analysis is given in another paper of the authors (Kypke and Langford 2020), for a slightly different EBM, that is our paleoclimate model. The present paper extends that analysis to the Anthropocene.

13. The model presented in this paper is just a first step in a program of research that eventually will combine the surface – atmosphere energy balance assumptions of this model with the convective flow of the Navier-Stokes-Boussinesq spherical shell model as in [Lewis and Langford (2008)]. Greg Lewis still has the code for that convection model, so it will be relatively easy to add energy balance from this model, to determine meridional surface temperatures implicitly. Greg has already proven the existence of a cusp bifurcation in that PDE model. Another goal is to adapt an open source model, such as perhaps PLASIM to our goals, in particular the goal of finding bistability and bifurcations, and then to compare the results.

14. Code availability: We are currently investigating our options in providing the code for our results in an online repository.

3 Author's changes in manuscript

The authors are mathematicians, and are well aware of the fact that they are novices in the field of climate science. The care and time given by the two referees, to better position this work in the climate change literature, is very much appreciated by the authors. The referees' suggestions in this regard have all been incorporated in the manuscript, in the manner indicated point-by-point in Section 2, above.

The confusing asymmetry, using T_S in Eq. (1) but I_A in Eq. (2), has been explained in the text, in the paragraph following Eq.s (1) and (2), and further explained in the derivation of Eq. (6). By "freeing" T_A to vary with altitude, the authors were enabled to use the atmospheric temperature dependence with height as given by the *lapse rate* of the ICAO International Standard Atmosphere. Since H_2O concentration varies with temperature, this allows a much more accurate determination of the greenhouse effect of water vapour. This choice is a significant improvement of the present EBM over previous EBMs in the literature.

Equations (10) and (22) for f_C and F_C have been simplified, as requested by Referee 1. Since F_C is only a minor contributor to the energy balance, a high degree of precision in its formulation is not necessary.

The change in the formula for F_C resulted in minor changes in some of the Figures. These have been recomputed. All figures have been configured to follow Copernicus guidelines.

The relation between Fig. 6(a) and Fig.s AI.8 and AI.9 in IPCCC AR4 has been clarified. Both use the four RCPs of Fig. 4 to determine hypothetical CO_2 concentrations (μ) by year, out to year 2100. Then both use these CO_2 concentrations as input to the model (EBM or GCM) to determine predicted climate changes. The agreement between EBM and GCM predictions is good. This agreement lends confidence to the use of this EBM for climate change predictions to the year 2300.

Referee 2 highlights several sentences in the manuscript that appear to disparage previous contributions to the field, saying these were "lacking in mathematical rigour" or did not provide "useful" contributions. These statements have been removed in the revised manuscript. Instead, new citations have been added, which exhibit both rigour and useful contributions.

The meaning of the vertical arrows, indicating transitions in Figures 6, 7 and 10, has been better explained in the Figure captions and the text.

We have designated the results quoted from the IPCC AR4 as "reports" rather than "predictions", as pointed out by Referee 2.

All of the papers cited by the referees have been added to the bibliography of the paper, along with statements in the paper which position them relative to the present work. Other relevant citations have been added as well, for a bibliography that now has 20 additional references, out of a total of 75.

In order to accommodate the two-column format, the figure pairs have been repositioned vertically instead of horizontally.

Following the Copernicus style instructions, we have used abbreviations Eq. and Fig. for equations and figures.

The "Conclusions" section has been expanded to better describe future work. The "Author Contribution" and "Competing Interests" sections have been completed.

The computer code used to produce the Figures of this manuscript has been made available on the zenodo website, as cited in the manuscript.

A complete listing of changes in the manuscript, generated by the software latexdiff, follows this Authors' Response.

Anthropocene ~~Climate Bifurcation~~climate bifurcation

Kolja Leon Kypke, William Finlay Langford, and Allan Richard Willms

Department of Mathematics and Statistics, University of Guelph, 50 Stone Road West, Guelph, ON, Canada N1G 2W1

Correspondence: William F. Langford (wlangfor@uoguelph.ca)

Abstract. This article presents the results of a bifurcation analysis of a simple Energy Balance Model (EBM) for the future climate of the Earth. The main focus is on the question: Can the nonlinear processes intrinsic to atmospheric physics, including natural positive feedback mechanisms, cause a mathematical bifurcation of the climate state, as a consequence of continued anthropogenic forcing by rising greenhouse gas emissions? Our analysis shows that such a bifurcation could cause an abrupt change, to a drastically different climate state in the EBM, warmer and more equable than any climate existing on Earth since the Pliocene Epoch. In previous papers, with this EBM adapted to paleoclimate conditions, it was shown to exhibit saddlenode and cusp bifurcations, as well as hysteresis. The EBM was validated by the agreement of its predicted bifurcations with the abrupt climate changes that are known to have occurred in the paleoclimate record, in the Antarctic at the Eocene-Oligocene Transition (EOT) and in the Arctic at the Pliocene-Paleocene Transition (PPT). In this paper, the EBM is adapted to fit Anthropocene climate conditions, with emphasis on the Arctic and Antarctic climates. The four Representative Concentration Pathways (RCP) ~~developed~~ considered by the IPCC are used to model future CO_2 concentrations, corresponding to different scenarios of anthropogenic activity. In addition, the EBM investigates four naturally occurring nonlinear feedback processes which magnify the warming that would be caused by anthropogenic CO_2 emissions alone. These four feedback mechanisms are: ice-albedo feedback, water vapour feedback, ocean heat transport feedback and atmospheric heat transport feedback. The EBM predicts that a bifurcation resulting in a catastrophic climate change, to a pre-Pliocene-like climate state, will occur in coming centuries ~~,~~for an RPC with unabated anthropogenic forcing, amplified by these positive feedbacks. However, the EBM ~~suggests~~ also predicts that appropriate reductions in carbon emissions may limit climate change to a more tolerable continuation of what is observed today. ~~This~~ The globally-averaged version of this EBM has an Equilibrium Climate Sensitivity (ECS) of 4.34 K, near the high end of the ~~range recorded~~ likely range reported by the IPCC.

---

1 Introduction

Today, there is widespread agreement that the climate of the Earth is changing, but the precise trajectory of future climate change is still a matter of debate. Recently there has been much interest in the possibility of ~~tipping points~~ “tipping points” (or bifurcation points) ~~causing~~ at which occur abrupt changes in the ~~evolution of the~~ Earth climate system~~, see (Alley et al. (2003); Seager and Battisti (2007); Lenton et al. (2008); Dit~~
~~)~~; see Brovkin et al. (1998); Ghil (2001); Alley et al. (2003); Seager and
. Section 12.5.5 in ~~(IPCC (2013))~~ IPCC (2013) gives an overview of such potential abrupt changes. At such points, a small change in the forcing parameters (whether anthropogenic or natural forcings) may cause a catastrophic change in the state of the system. In order to prepare for future climate change, it is of great importance to know if such abrupt changes can occur, and if so, when and how they will occur. ~~It has been~~ Some authors have suggested that conventional General Circulation Models (GCM) may be “too stable” to provide reliable warning of these sudden catastrophic events ~~(Valdes (2011)), but~~ (Valdes, 2011), and that the study of paleoclimates may be a better guide to how abrupt changes may occur ~~(Zeebe (2011)).~~ (Zeebe, 2011). Steffen et al. (2018) asked the fundamental question: “Is there a planetary threshold in the trajectory of the Earth System that, if crossed, could prevent stabilization in a range of intermediate temperature rises?”

In this paper, a simple Energy Balance Model (EBM) is used to investigate the ~~possibility of such sudden catastrophic events.~~

possible occurrence of such a threshold (or tipping point or bifurcation point) in the climate of the Anthropocene. Energy Balance Models assume that the climate is in an equilibrium state, for which "energy in equals energy out" at each point of the Earth's surface and atmosphere. Thus, time-dependence is eliminated from the model, greatly simplifying the analysis. In the literature, EBMs have played an important role in understanding climate and climate change ~~(Budyko (1968); Sellers (1969); Sagan and Mullen (1972); North et al. (1981); Thorndike (2012); Kaper and Engler (2013); Dijkstra (201). Often these EBMs do exhibit bifurcations, but may be lacking in the geophysical details and the mathematical rigour required to make useful predictions. This~~ (Budyko, 1968; Sellers, 1969; Sagan and Mullen, 1972; North et al., 1981; Thorndike, 2012; Kaper and Engler, 2013; Dijkstra, 2013; Pay . Many of those EBMs have exhibited bifurcations. The present paper presents an EBM ~~built upon~~ with more accurate diagnostic equations than the early EBMs, built upon the basic laws of geophysics ~~, which determine nonlinear positive~~ and including nonlinear feedback processes that amplify anthropogenic CO_2 forcing~~and may lead to bifurcations. A~~ . A rigorous mathematical bifurcation analysis of this EBM ~~applied to paleoclimate changes was presented in (Kypke (2019); Kypke and Langford (2020))~~has been presented in Kypke and Langford (2020). That analysis gave a mathematical proof of the existence of a cusp bifurcation in the EBM, complete with a determination of the Center Manifold and of the universal unfolding parameters, as functions of the relevant physical parameters. The existence of the cusp bifurcation implies the co-existence of two distinct stable equilibrium climate states (bistability), as well as the existence of ~~abrupt~~ hysteresis; that is, two abrupt one-way transitions between these two states (via fold bifurcations) exist in the EBM. ~~These transitions are dependent on the past history of the system (hysteresis). In addition, the two universal unfolding parameters for the cusp bifurcation were determined as functions of the relevant physical parameters~~The present paper extends those results from the paleoclimate model in Kypke and Langford (2020) to the Anthropocene climate model studied here. This Anthropocene model gives predictions of climate changes in the 21st century and beyond.

One advantage of an EBM over a more complex GCM is that it facilitates the exploration of specific cause and effect relationships, as particular climate forcing factors are varied or ignored. Another advantage of an EBM is that rigorous mathematical analysis often can prove the existence of certain behaviours, such as bistability and bifurcations, that could only be surmised from numerical evidence, or missed, in more complicated models. Four versions of the EBM are considered here: a globally averaged temperature model and three regional models corresponding to Arctic, Antarctic and Tropical climates.

This EBM was validated in ~~(Dortmans et al. (2019); Kypke and Langford (2020))~~Dortmans et al. (2019), where it was applied to known paleoclimate changes. It successfully "predicted" the abrupt glaciation of Antarctica at the Eocene-Oligocene transition (EOT) and the abrupt glaciation of the Arctic at the Pliocene-Pleistocene transition ~~, using a~~ (PPT), using bifurcation analysis. ~~Those paleoclimate bifurcations led to~~ The transitions in the model were congruent with the abrupt cooling, from warm, equable "hothouse" climate conditions to a cooler state like the climate of today, with ice-capped poles, as indelibly recorded in the geological record at the EOT and PPT.

~~This paper applies that~~ In adapting the previous paleoclimate EBM to the ~~Earth's~~ climate of the Anthropocene~~. It~~ , this paper explores the possibility of a "reversal" of those two paleoclimate ~~bifurcations, which may (or may not) occur in future centuries,~~ transitions; that is, a transition from today's climate with ice-capped poles to an equable hothouse climate state, such as existed in the Pliocene and earlier. It provides new mathematical evidence ~~signifying~~ suggesting that catastrophic climate change in polar regions is inevitable in the coming decades and centuries, if current anthropogenic forcing continues unabated. The EBM also suggests that ~~mitigation strategies exist, which can avoid~~ if appropriate mitigation strategies are adopted (as recommended by the IPCC), such an outcome can be avoided.

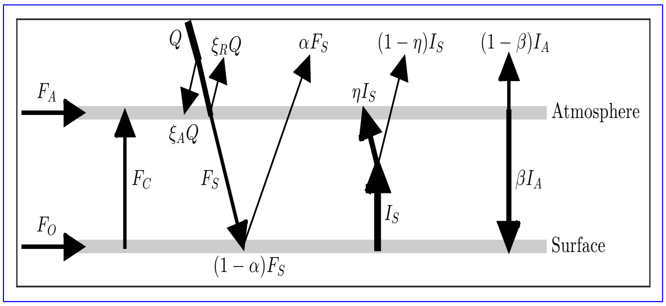

Figure 1. A visualization of the energy balance model (EBM). Here Q is the incident solar radiation. A fraction ξ_A of Q is absorbed by the atmosphere and another fraction ξ_R is reflected by clouds into space. The resulting solar forcing that strikes the surface is $F_S = (1-\xi_A-\xi_R)Q$. The surface has albedo α, which means that αF_S is reflected back to space and the remaining energy $(1-\alpha)F_S$ is absorbed by the surface. The surface emits longwave radiation of intensity I_S, of which a fraction ηI_S is absorbed by greenhouse gases in the the atmosphere and the remainder $(1-\eta)I_S$ escapes to space. The atmosphere emits longwave radiation I_A, of which a fraction βI_A goes downward to the surface and the remaining fraction $(1-\beta)I_A$ escapes to space. The three forcing terms F_A, F_O, F_C represent atmospheric heat transport, ocean heat transport and vertical conduction/convection heat transport, respectively. Values of these and other parameters are given in Table 1.

The EBM of this paper has been kept as simple as possible, while incorporating the nonlinear physical processes that are essential to our exploration of bifurcation behaviour. In that sense, it follows in the tradition of simple energy balance models of Budyko (1968); Sellers (1969); North et al. (1981) and others. However, this EBM is but the first step in the authors' study of a hierarchy of nonlinear models of increasing complexity. That hierarchy is outlined in the concluding Section 4.

2 An ~~Energy Balance Model~~ energy balance model for ~~Climate Change~~climate change

The EBM is a simple two-layer model, with layers corresponding to the surface and atmosphere, respectively; see Fig. ~~??~~ 1, which is based on ~~(Payne et al. (2015); Trenberth et al. (2009); Wild et al. (2013))~~Payne et al. (2015); Trenberth et al. (2009); Wild et al. (2013). The symbols in Fig. ~~??~~ 1 are defined in the caption of Fig. ~~??~~ 1 and in Table 1. In the EBM of ~~Figure ??~~Fig. 1, the surface receives short-wave radiant energy ~~$F_S=(1-\xi_a-\xi_R)Q$~~ $F_S=(1-\xi_A-\xi_R)Q$ from the sun, where Q is the incident solar radiation ~~. and ξ_A,ξ_R~~ and ξ_A, ξ_R are the fractions of Q absorbed by the atmosphere and reflected back to space by clouds, respectively. The values of ξ_A and ξ_R are obtained from ~~(Trenberth et al. (2009); Wild et al. (2013))~~Trenberth et al. (2009); Wild et al. (2013), see the Appendix and Table 1. At the surface, a fraction αF_S is reflected back to space, where α is the surface albedo, and the ~~remainder~~ remainder $(1-\alpha)F_S$ is absorbed by the surface. The surface re-emits long wave radiant energy of intensity $I_S=\sigma T_S^4$ (~~Stephan-Boltzmann~~ Stefan–Boltzmann Law), upward into the atmosphere. The atmosphere contains greenhouse gases that absorb a fraction η of the radiant energy I_S from the surface, and the remainder $(1-\eta)I_S$ escapes to space. The atmosphere re-emits radiant energy of total intensity I_A. Of this radiation I_A, a fraction β is directed downward to the surface, and the remaining fraction $(1-\beta)$ goes upward and escapes to space.

Balancing the energy flows represented in Fig. ~~??~~ 1 leads directly to the following dynamical system

$$\begin{aligned} c_S\frac{dT_S}{dt} &= (1-\alpha)(1-\xi_A-\xi_R)Q+F_O+\beta I_A \\ &\quad -\sigma T_S^4-F_C, \qquad (1)\\ c_A\frac{dI_A}{dt} &= F_A+\eta\sigma T_S^4-I_A+F_C+\xi_A Q, \qquad (2)\end{aligned}$$

where (1) represents surface energy balance and (2) represents atmosphere energy balance. Here c_S and c_A are specific heat rate constants derived in ~~(Kypke (2019); Kypke and Langford (2020))~~ Kypke (2019); Kypke and Langford (2020) and listed in Table 1. There are three heat transport terms: F_A is *atmospheric* heat transport and F_O is *ocean* heat transport (both horizontally), and F_C is *conductive/convective* heat transport, vertically from the surface to the atmosphere.

In Eq.s (1) and (2) there is an asymmetry, in that temperature T_S is used to represent the state of the surface in (1), but radiant energy intensity I_A is used instead of temperature to represent the state of the atmosphere in (2). Note that either temperature or energy intensity variables could have been used in either equation, if we assume the Stefan–Boltzmann Law ($I_S=\sigma T_S^4$ and $I_A=\epsilon\sigma T_A^4$, where $\epsilon=0.9$ is the emissivity of dry air). The use of T_S as state variable in surface Eq. (1) is the obvious choice, since the surface temperature is the most important variable in the EBM. However, the choice of I_A instead of T_A in (2) is less obvious. The atmosphere has thickness. In the actual atmosphere, temperature decreases with height above the surface, at a rate called the *lapse rate*. Therefore, there is not just one value of temperature T_A for the atmosphere. However, we can define a single value of radiant energy intensity I_A, corresponding to the total energy emitted vertically by the slab of atmosphere, and use this instead of temperature in the energy balance Eq. (2). A second reason for the use of I_A instead of T_A in Eq. (2) is that this facilitates the use of the ICAO Standard Atmosphere lapse rate, as explained in the paragraph following the Eq.s (4) and (5) below, and that allows a more realistic representation of the greenhouse gas behaviour of water vapour.

The first step of the analysis of system (1)(2) is a rescaling of temperature T (in degrees Kelvin) to a new non-dimensional temperature τ with $\tau=1$ corresponding to the freezing temperature of water ($T_R=273.15$ K). Then all variables and parameters in the system can be made non-dimensional by the scalings

$$\begin{aligned} &\tau_A=\frac{T_A}{T_R},\quad \tau_S=\frac{T_S}{T_R},\quad q=\frac{Q}{\sigma T_R^4},\quad f_O=\frac{F_O}{\sigma T_R^4},\\ &f_A=\frac{F_A}{\sigma T_R^4},\quad f_C=\frac{F_C}{\sigma T_R^4},\quad i_A=\frac{I_A}{\sigma T_R^4},\quad \omega=\frac{\Omega}{T_R}, \qquad (3)\\ &s=\frac{\sigma T_R^3}{C_S}\cdot t,\quad \chi=\frac{C_S}{C_A\sigma T_R^3}=54.26,\end{aligned}$$

where s is dimensionless time and χ is the dimensionless heat rate constant. The surface and atmosphere energy balance ~~equations~~ Eq.s (1)(2) in non-dimensional variables are then

$$\begin{aligned} \frac{d\tau_S}{ds} &= (1-\alpha(\tau_S))(1-\xi_A-\xi_R)q\\ &\quad +f_O+\beta i_A-\tau_S^4-f_C, \qquad (4)\\ \frac{1}{\chi}\frac{di_A}{ds} &= f_A+\eta(\tau_S;\mu,\delta)\tau_S^4-i_A+f_C+\xi_A q. \qquad (5)\end{aligned}$$

~~The atmosphere in~~ In Fig. ~~?? is assumed~~ 1, the atmosphere is shown to be a uniform slab, even though the actual atmosphere is not a uniform slab. ~~However, the~~ The essential nonlinear processes in the atmosphere, which the model must capture, are the heating effects of the greenhouse gases CO_2 and H_2O. According to the Beer-Lambert law, the absorptivity of these gases is determined by their *optical depths*. Therefore, in the model we substitute for optical depth in the slab, the values of optical depth that these gases would have in the International Standard Atmosphere ~~(ICAO (1993))~~(ICAO, 1993), which is a good approximation to the actual atmosphere. In ~~this case~~the ICAO model, the rate of change of temperature with altitude is assumed to be a negative constant $-\Gamma$, called the ICAO *lapse rate*, see Table 1. The concentration of CO_2 is independent of temperature, but the concentration of H_2O decreases with altitude as the temperature decreases, according to the Clausius-Clapeyron relation ~~(Pierrehumbert (2010)).~~ (Pierrehumbert, 2010). Then the optical depth of H_2O is obtained by integration of the Clausius-Clapeyron relation from the surface to the tropopause, ~~as seen~~ resulting in (6). In this way, the simple ~~two-layer~~ slab model has greenhouse effects close to those of these two gases in the actual atmosphere~~. For further details see (Dortmans et al. (2019)). Thus, in the atmosphere equation or , the total~~ , where the temperature is not constant but decreases with altitude. This use of the ICAO lapse rate differentiates the present EBM from all previous EBMs in the literature. The calculation gives the absorptivity η due to greenhouse gases~~is determined~~ , in the atmosphere Eq. (2) or (5), as

$$\eta(\tau_S;\mu,\delta) = 1-\exp\Bigg[-\mu G_c-\delta G_{W2}\cdot \int\limits_{\tau_S-\gamma Z}^{\tau_s}\frac{1}{\tau}\exp\left(G_{W1}\left[\frac{\tau-1}{\tau}\right]\right)d\tau\Bigg], \tag{6}$$

where μ is the concentration of CO_2 in the atmosphere, measured in molar parts per million, δ is the relative humidity of water vapour ($0\leq\delta\leq 1$), $\gamma=\Gamma/T_R$ is the nondimensionalized lapse rate ~~(ICAO (1993))~~(ICAO, 1993), and Z is the tropopause height. (Since methane acts similarly to carbon dioxide as a greenhouse gas, it may be assumed that μ includes also the effects of methane.) Equation (6) is derived using fundamental laws of atmospheric physics: the Beer-Lambert law, the ideal gas law and the Clausius-Clapeyron equation, see ~~(Dortmans et al. (2019)) for~~ Dortmans et al. (2019) for more details. In ~~equation~~ Eq. (6),

$$G_c=\frac{1.52k_cP_A}{10^6g},\quad G_{W1}=\frac{L_v}{R_WT_R},\quad \text{and}\quad G_{W2}=\frac{k_W\cdot T_R\cdot\rho^{sat}(T_R)}{\Gamma}, \tag{7}$$

are dimensionless physical constants determined in ~~(Dortmans et al. (2019))~~ Dortmans et al. (2019), and k_C, k_W are absorption coefficients for CO_2 and H_2O respectively; see Table 1. ~~Equation determines the total greenhouse warming effects of CO_2 and H_2O, for given μ and δ, and temperature τ_S.~~

In the surface ~~equation~~ Eq. (1) or (4), α is the albedo of the surface ($0\leq\alpha\leq 1$), and α depends strongly on temperature ~~τ~~ τ_S near the freezing point ~~$\tau=1$~~($\tau_S=1$). Typical values of surface albedo are: 0.6–0.9 for snow, 0.4–0.7 for ice, 0.2 for crop land and 0.1 or less for open ocean. Therefore, in the high Arctic, as the ice-cover melts, the albedo will transition from a high value such as $\alpha_c=0.7$ for snow/ice, to a low value such as $\alpha_w=0.08$ for open ocean. Some authors have assumed this change in albedo to be a discontinuous step function ~~(Dortmans et al. (2018))~~(Dortmans et al., 2018). However, all variables in this EBM have annually averaged values. As the Arctic thaws, the annual average albedo will transition gradually, over a number of years, from its high value for year-round ice-covered surface to its low value for year-round open ocean. Therefore, in this paper we use a smoothly varying albedo function, which better models this gradual transition from high to low albedo, as the mean temperature rises through the freezing point ($\tau_S=1$). It is modelled by the hyperbolic tangent function:

$$\alpha(\tau_S,\omega)=\frac{1}{2}\left([\alpha_w+\alpha_c]+[\alpha_w-\alpha_c]\tanh\left(\frac{\tau_S-1}{\omega}\right)\right). \tag{8}$$

Here the parameter ω controls the steepness of this switch function. Analysis of polar ice data in recent years confirms that this function gives a good fit to the decline of ice cover and albedo in the Arctic with $\omega=\Omega/T_R=0.01$ ~~(Dortmans et al. (2019))~~(Pistone et al., 2014; Dortmans et al., 2019). The dependence of Arctic Ocean sea ice thickness on surface albedo parametrization in models has been investigated in ~~(Björk et al. (2013))~~Björk et al. (2013), where alternative albedo schemes are compared. The nonlinear dependence of albedo on temperature, as in (8), has been shown to lead to ~~*hysteresis* behaviour (Stranne et al. (2014); Dortmans et al. (2019)).~~

~~Previous papers (Dortmans et al. (2019); Kypke and Langford (2020)) used the EBM to investigate transitions in paleoclimates; in particular the Eocene-Ologocene Transition (EOT) and the Pliocene-Pleistocene Transition (PPT). In addition to shedding light on the underlying causes of those transitions, the agreement achieved in those papers has served as a validation of the EBM, and of the fundamental hypothesis that bifurcations can occur in the Earth climate system~~hysteresis behaviour (Stranne et al., 2014; Dortmans et al., 2019).

2.1 Refinement of the Paleoclimate EBM to an Anthropocene EBM

Paleoclimate data are difficult to obtain and in general can only be inferred from proxy data. The situation is different for the Anthropocene. There is now an abundance of land-based and satellite climate data. Therefore, the EBM in this paper can be refined to take advantage of the additional data. The Appendix details the changes made in ~~the~~ this EBM, from that which was presented in ~~(Dortmans et al. (2019); Kypke and Langford (2020))~~Dortmans et al. (2019); Kypke and Langford (2020), to improve its accuracy for the Anthropocene. These changes do not change the fundamental behaviour of the EBM, including the existence of bifurcations, but they do make the numerical predictions more reliable. Table 1 of this paper may be compared with the corresponding Table 1 of ~~(Kypke and Langford (2020))~~Kypke and Langford (2020), to see how parameter values have been updated.

The total absorptivity η, given in (6) for paleoclimates, is ~~modified,~~ now modified to reflect the fact that clouds absorb a fraction η_{Cl} of the outgoing longwave radiation~~,~~. In this paper

$$\eta(\tau_S,\mu,\delta) = 1-(1-\eta_{Cl})\cdot\exp\left[-\mu G_c-\delta G_{W2}\cdot\int_{\tau_S-\gamma Z}^{\tau_s}\frac{1}{\tau}\exp\left(G_{W1}\left[\frac{\tau-1}{\tau}\right]\right)d\tau\right], \tag{9}$$

see the Appendix.

The vertical heat transport term F_C has been modified to take into account both sensible and latent heat transport ~~(Kypke (2019)) see~~ (Kypke, 2019). See the Appendix, where the following formula is obtained (here in nondimensional form).

$$f_C(\tau_S) = \frac{H_1\gamma Z}{(\tau_S-\gamma Z)}+\frac{H_2}{(\tau_S-\gamma Z)}\cdot\left(e^{\left[G_{W1}\frac{\tau_S-1}{\tau_S}\right]}-\delta e^{\left[G_{W1}\frac{\tau_S-\gamma Z-1}{\tau_S-\gamma Z}\right]}\right), \tag{10}$$

~~In equations , at equilibrium (i.e. $\frac{d\cdot}{d\hat{s}}=0$), the state variable i_A is easily eliminated, leaving a single equation with a single state variable τ_S~~where H_1 and H_2 are nondimensional constants,

$$H_1=\frac{C_DUc_PP_0}{\sigma T_R^4R_A} \quad\text{and}\quad H_2=\frac{C_DUL_vP^{sat}(T_R)}{\sigma T_R^5R_W}.$$

In Eq.s (4)(5), at equilibrium (i.e. $\frac{d\cdot}{d\hat{s}}=0$), the state variable i_A is easily eliminated, leaving a single equation with a single state variable τ_S,

$$\begin{aligned}0 \;=\;& (1-\alpha(\tau_S))(1-\xi_A-\xi_{Cl})q+f_O+\beta f_A\\ &-f_C(1-\beta)+\beta q\xi_A-\tau_S^4(1-\beta\eta(\tau_S)).\end{aligned} \tag{11}$$

2.2 Cusp ~~Bifurcation~~ bifurcation in the EBM

In this subsection, we outline the proof that the cusp bifurcation, which was proven to exist in the Paleoclimate EBM ~~(Kypke and Langford (2020))~~(Kypke and Langford, 2020), in fact persists in this Anthropocene EBM (4)(5). Therefore, the conclusions of that paper carry over to this paper. Readers not interested in these mathematical details may skip this subsection.

The right hand sides of (4)(5), can be represented by a single vector function $F:\mathbb{R}^2\times\mathbb{R}^4\to\mathbb{R}^2$. Then an equilibrium point $(\bar{\tau}_S,\bar{i}_A)$ of (4)(5), at which $\frac{d\tau_S}{dt}=\frac{di_A}{dt}=0$, is a solution of , ~~where ρ represents four physical parameters that may be varied in the model,~~

$$F(\bar{\tau}_S,\bar{i}_A;\rho)=0, \tag{12}$$

where ρ represents four physical parameters that may be varied in the model,

$$\rho\equiv\{\mu,\delta,F_O,\omega\}. \tag{13}$$

See Table 1 for definitions of these parameters. Since the codimension of the cusp bifurcation is only two, there is some redundancy in the choice of these four parameters. For application to future climates, the parameter pair (F_O,μ) is of primary ~~importance~~interest. Equilibrium points $(\bar{\tau}_S,\bar{i}_A)$ satisfying (12) have been computed in ~~(Kypke (2019))~~Kypke (2019). Having computed the equilibrium point $(\bar{\tau}_S,\bar{i}_A)$ satisfying (12), the system may be translated to the origin $(x,y)=(0,0)$, in new state variables defined by ~~and equations become~~

$$(x,y)\equiv(\tau_S-\bar{\tau}_S,i_A-\bar{i}_A),$$

and Eq.s (4)(5) become

$$\begin{aligned}\frac{dx}{ds}&=(1-\alpha)(1-\xi_A-\xi_{Cl})q+f_O-f_C\\ &\qquad+\beta(y+\bar{i}_A)-(x+\bar{\tau}_S)^4,\\ \frac{dy}{ds}&=\chi\left[f_A+f_C+q\xi_A+\eta(x+\bar{\tau}_S)^4-(y+\bar{i}_A)\right].\end{aligned} \tag{14}$$

In order that 14 have a steady-state bifurcation at the equilibrium point ~~(0.0)~~(0, 0), the Jacobian J of F in (12) must have a zero eigenvalue $\lambda_1=0$ at that point. (A Hopf bifurcation is not possible in this system.) For stability, the second eigenvalue satisfies $\lambda_2<0$. The corresponding eigenvectors $\mathbf{e}_1,\mathbf{e}_2$ form an *eigenbasis*. A linear transformation takes (x,y) coordinates to *eigenbasis coordinates* (u,v), where $(x,y)=T(u,v)$, and the columns of T are the normalized eigenvectors $\mathbf{e}_1,\mathbf{e}_2$ in (17), below. Then in (u,v) coordinates, the 2D system (14) becomes

~~where~~

$$\begin{aligned}\frac{du}{ds} &= \frac{1}{\phi}\Big[(1-\alpha)(1-\xi_A-\xi_{Cl})q+f_O+\beta f_A \qquad (15)\\ &- (1-\beta)f_C+\beta\xi_A q+(1-\beta\eta)(u-kv+\bar{\tau}_S)^4\Big]\\ \frac{dv}{ds} &= \frac{1}{\phi}\Big[-\ell[(1-\alpha)(1-\xi_A-\xi_{Cl})q+f_O]\\ &+ (\ell+\chi)f_C+\chi f_A-(\ell\beta+\chi)[\ell u+v+\bar{\iota}_A]\\ &+ (\ell+\chi\eta)(u-kv+\bar{\tau}_S)^4\Big],\end{aligned}$$

where

$$\ell = f'_{C0}+4\eta_0\bar{\tau}_S^3+\eta'_0\bar{\tau}_S^4, \quad k=\frac{\beta}{\chi}, \quad \phi = 1+k\ell \qquad (16)$$

and

$$\mathbf{e}_1 = \begin{pmatrix}1\\ \ell\end{pmatrix}, \quad \mathbf{e}_2 = \begin{pmatrix}-k\\ 1\end{pmatrix}. \qquad (17)$$

Recall that the parameters μ and δ, representing CO_2 concentration and water vapour relative humidity, respectively, enter into Eq.s (15) through the function η defined in Eq. (9). For more details, see ~~(Kypke (2019); Kypke and Langford (2020); Kuznetsov (2004))~~Kypke (2019); Kypke and Langford (2020); Kuznetsov (2004) .

If the *Centre Manifold Theorem* applies to (15), then there exists a flow-invariant centre manifold, tangent to the u-axis. The applicability of this theorem has been verified, and the centre manifold has been computed, for the present Anthropocene EBM as was done ~~in (Kypke (2019); Kypke and Langford (2020))~~ for the paleoclimate EBM in Kypke (2019); Kypke and Langford (2020). Details are omitted here. A phase portrait for (15) in a neighbourhood of the cusp equilibrium point, together with a portion of this centre manifold (in red), is shown in ~~Figure ??~~ Fig. 2 in (u,v) coordinates. In this figure, trajectories quickly collapse to the centre manifold around the equilibrium point $(0,0)$, as predicted by the Centre Manifold Theorem. The cusp equilibrium manifold for (15) in normal form is shown in ~~Figure ??. Here β_1,β_2~~ Fig. 3. Here ζ_1,ζ_2 are the normal form unfolding parameters for the cusp bifurcation. Note the co-existence of three equilibrium points with different values of u (two stable and the middle one unstable) inside the ~~wedge-shaped~~ cusp-shaped region, but only one equilibrium point (stable) outside of that region.

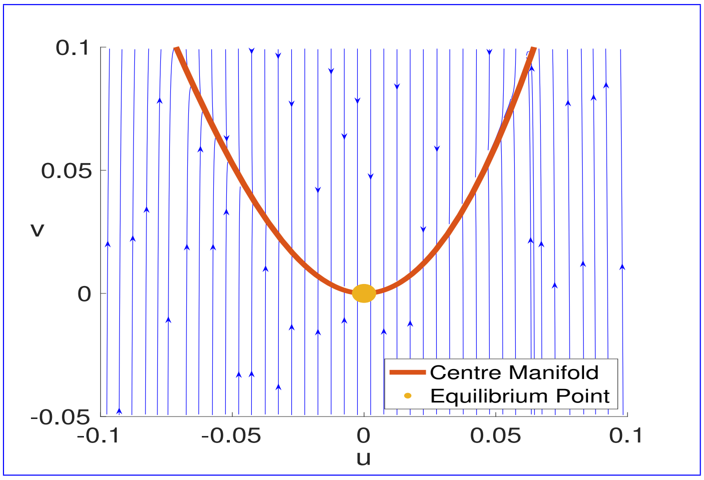

Figure 2. Phase portrait of system (15), together with a portion of the centre manifold (in red), in the (u,v) eigenbasis coordinates. Parameter values are those at the computed cusp point. The yellow dot marks the cusp equilibrium point. Note the rapid approach to the centre manifold from initial points not on the centre manifold, in contrast to the slow evolution along the centre manifold.

3 Anthropocene ~~Climate Forecasts~~climate forecasts

In this ~~section~~Section, the EBM of Section 2 is applied to ~~future climates~~ the present and future climates of the Earth, to investigate the possibility of climate bifurcations (or “tipping points”) in the Anthropocene. The principal parameters chosen to be explored are carbon dioxide concentration μ, ocean heat transport F_O and relative humidity δ. The EBM is adapted locally to three separate regions, namely the Arctic, Antarctic and Tropics, in subsections 3.2, 3.3 and 3.4, respectively.

Carbon dioxide production due to human activities has been well documented as a driver of climate change in the Anthropocene. Projections of future atmospheric CO_2 levels are available ~~,~~ under various future scenarios~~(IPCC (2013))~~; we follow the Representative Concentration Pathways of IPCC (2013), described in subsection 3.1. Ocean heat transport is a difficult quantity to predict, as many different factors influence the transport of heat to various regions of the world via the oceans. Changes in temperature can change ocean heat transport which in turn ~~positively affects temperature~~affects local temperatures. This is ocean heat transport feedback, which is explored in subsection 3.2.2. Similarly, the role of atmospheric heat transport feedback is investigated briefly in subsection 3.2.2. In addition, water vapour is a powerful greenhouse gas, with a positive feedback effect that is investigated in subsection 3.2.3.

~~The EBM is adapted to three separate regions, namely the Arctic, Antarctic and Tropics. A~~ In subsection 3.5, a globally-averaged model ~~also~~ is considered, mainly for the purpose of determining the global Equilibrium Climate Sensitivity (ECS) of this EBM, for comparison with ~~that~~ the ECS of other models ~~,~~ as reported in ~~(IPCC (2013)); see Section~~IPCC (2013); Priostosescu and Huybers (2017) ; see subsection 3.6.

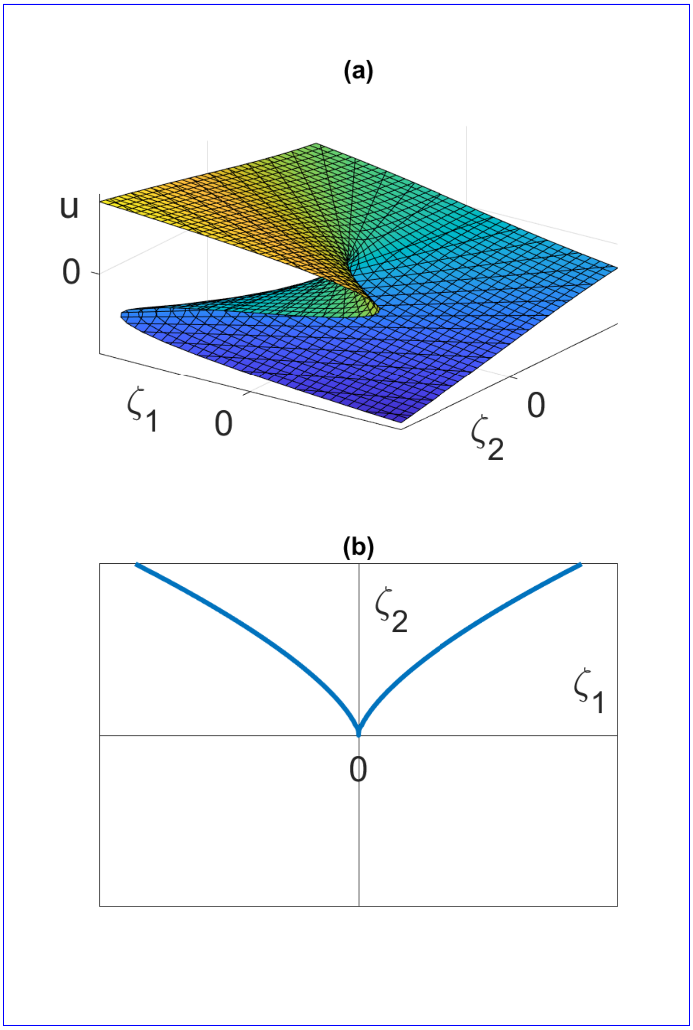

Figure 3. Cusp bifurcation diagram for the EBM in normal form coordinates. (a) Graph of the equilibrium surface with normal form unfolding parameters (ζ_1, ζ_2). (b) Projection of this surface in 3D onto the (ζ_1, ζ_2) plane. The blue semi-cubic parabola represents fold bifurcations, and it separates the (ζ_1, ζ_2) plane into two open 2D regions. Inside the *~~wedge region~~cusp region*, that is between the two branches of the semi-cubic parabola, there exist three equilibrium solutions u, two stable and the middle one unstable. Outside of the semi-cubic parabola there exists only one unique equilibrium solution u and it is stable.

3.1 Representative ~~Concentration Pathways~~ concentration pathways (RCP)

The IPCC has ~~developed~~ standardized on four Representative Concentration Pathways (RCP), which are used for projections of future carbon dioxide concentrations; see van Vuuren et al. (2011) and Box TS.6 in ~~(IPCC (2013))~~IPCC (2013). These RCPs are scenarios for differing levels of anthropogenic forcings on the climate of the Earth and represent differing global societal and political "storylines". The scenarios are named RCP 8.5, RCP 6.0, RCP 4.5 and RCP 2.6, after their respective peak radiative forcing increases in the 21st century. That is, in the year 2100, RCP 8.5 will reach its maximum radiative forcing due to anthropogenic emissions of $+8.5$ W/m^2 relative to the year 1750. This scenario is understood as one where emissions continue to rise and are not mitigated in any way. RCP 6.0 corresponds to $+6.0$ W/m^2 and RCP 4.5 corresponds to $+4.5$ W/m^2 relative to 1750. These are stabilization scenarios, where greenhouse gas emissions level off to a target amount by the end of the century. Finally, RCP 2.6 corresponds to $+2.6$ W/m^2 in 2100, relative to 1750. This is a mitigation scenario, where strong steps are taken to eliminate the increase, and eventually reduce, anthropogenic greenhouse gas emissions. Figure~~??~~ 4 shows the carbon dioxide concentrations, projected to the year 2500 in the IPCC scenarios for the four RCPs. The carbon dioxide increase is relatively moderate for RCPs 2.6 and 4.5, even decreasing eventually for RCP 2.6. The increase for RCP 6.0 is larger, and it is drastic for RCP 8.5.

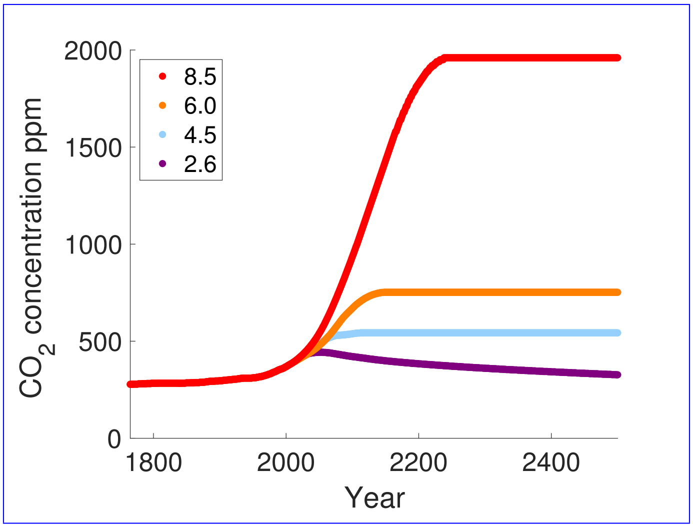

Figure 4. Carbon Dioxide concentration μ, as projected by the IPCC for each of the four RCP hypothetical scenarios. This figure is generated from data at ~~(IIASA (2019))~~IIASA (2019).

~~The~~ These RCPs represent hypothetical ~~forcing~~ forcings due to human activity up to the year 2100. Beyond 2100, they assume a "constant composition commitment", where emissions are kept constant, which serves to stabilize the scenarios beyond 2100 ~~(IPCC (2013))~~(IPCC, 2013). Of course, emissions could continue to increase, or be greatly reduced ("zero emissions commitment") at some point in the future. However, the constant emission commitment dataset provided in ~~(IPCC (2013))~~IPCC (2013), and shown in ~~Figure ??~~Fig. 4, is what is utilized in this work. In the following sections we enter the CO_2 concentrations μ shown in Fig. 4, one at a time along each of the four IPCC RCPs~~into the various~~, into the versions of our EBM for the Arctic, Antarctic, etc., and then let the ~~climate evolve along each~~

~~of the~~ EBM climate evolve quasi-statically along each CO_2 ~~pathways in Figure ??~~pathway.

3.2 EBM for the Anthropocene Arctic

Figure~~??~~ 5(a) is the manifold of equilibrium ~~points~~ states for the EBM parameterized by (F_O, μ), for the case of an Arctic climate under Anthropocene conditions. Figure~~??~~ 5(b) is the projection of this manifold onto the parameter plane, showing the fold bifurcation lines as boundaries between coloured regions. Parameter values are as in Table 1, with $F_A = 104$ W/m^2, and $\delta = 0.6$ taken as the nominal values for the modern Arctic throughout this Section, except in ~~Figure ??~~Fig. 8. These figures were computed as in ~~(Kypke and Langford (2020))~~Kypke and Langford (2020) . The cusp point, seen in ~~Figure ??~~Fig. 3, still exists but is not visible in ~~Figure ??~~Fig. 5, because it is outside of the range of parameters included in the figure.

In Figure~~??~~ 5(a), today's climate state lies on the lower (blue) portion of the equilibrium manifold, as shown by the red dot. The upper (yellow) portion represents a co-existing warm equable climate state, similar to the climate of Earth in the Pliocene and earlier. The intermediate (green) portion represents an unstable (and unobservable) climate state.

Similarly, in ~~Figure ??~~Fig. 5(b), the blue area represents unique cold stable states, yellow represents unique warm stable states, and the green region is the overlap region, between the two fold bifurcations, where both warm and cold states co-exist. Hence, on moving in the (F_O, μ) parameter space starting from the blue region, crossing the green region, and into the yellow region, there would be no observable change in climate on crossing from blue to green; however, crossing the boundary from green to yellow would cause a catastrophic jump from cold to warm stable climate states. Alternatively, if the (F_O, μ) parameter values moved from the yellow, through the green, into the blue region in ~~Figure ??~~Fig. 5(b), there would be no abrupt change in climate state on crossing the yellow/green boundary, but a sudden transition to a cold state would occur at the green/blue boundary. This behaviour is called *hysteresis*.

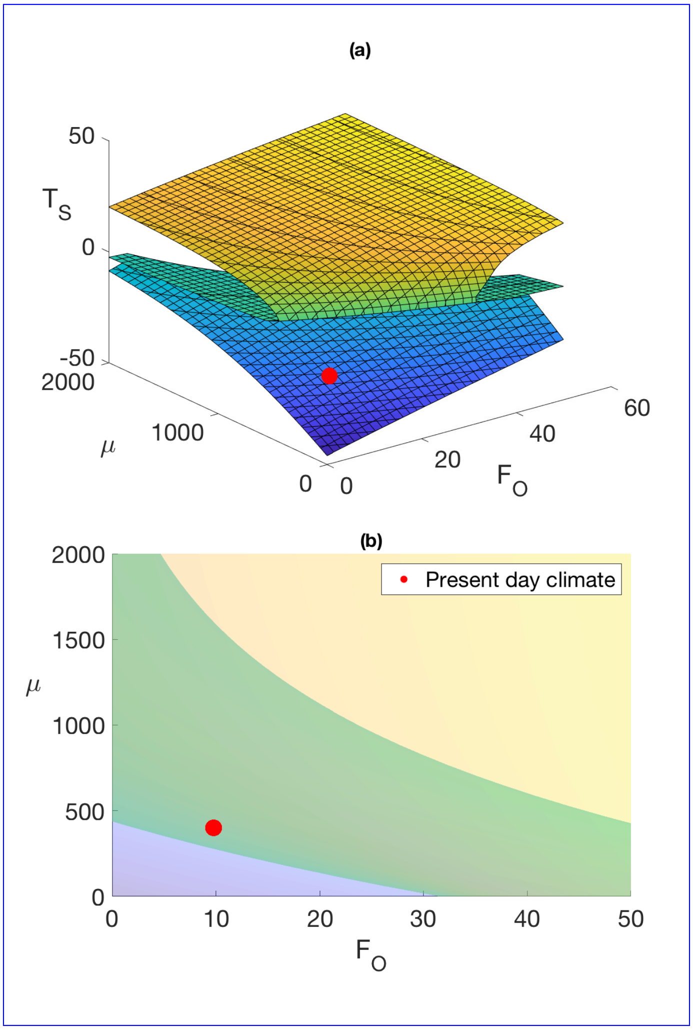

Figure 5. Energy Balance Model of the modern Arctic. Parameter values are as in Table 1. The red dots locate today's Arctic climate conditions. Ocean heat transport F_O increases from 0 to 50 W/m^2 and carbon dioxide concentration μ increases from 0 to 2000 ppm. (a) 3D plot of equilibrium manifold. (b) Projection on the (F_O, μ) parameter plane.

3.2.1 Arctic ~~Climate~~ climate for the 4 RCPs

The paramount question considered in this paper can now be phrased as follows. Can a bifurcation, leading to a ~~warm~~ warmer and more equable climate state ~~,~~ be expected in the EBM, if it is allowed to evolve along one of the four RPCs in ~~Figure ??? In Figure ??~~Fig. 4? In Fig. 5(b), this bifurcation would correspond to crossing the line of fold bifurcations separating the green and yellow regions, on increasing μ and possibly F_O.

Figure ~~??~~ 6 shows the increase in surface temperature ~~for~~ in the Arctic region~~for historical data starting in~~ , using historical data from the year 1900 ~~and EBM projections~~ to the present, and then the EBM forecasts up to the years 2100 and 2300, ~~on~~ holding μ to each of the four RPCs ~~,~~ in Fig. 4, and with constant F_O = 10 W/m^2, F_A = 104 W/m^2 and $\delta = 0.6$. The temperature change shown is relative to the Arctic temperature of the ~~model~~ EBM in the year ~~2000. This figure should~~ 2000, which was -28.90°C ($\tau_S = 0.8942$).

Figure 6 (a) may be compared to the results ~~seen in Figure AI.8~~ in ~~(IPCC (2013)).While that Figure~~ Fig.s AI.8 ~~provides~~ and AI.9 in IPCC (2013). Those figures use the RCPs of Fig. 4 and an ensemble of climate models to forecast surface temperature changes for the Arctic ~~, for both sea and land separately, and only for~~ up to the year 2100, for land and sea separately. IPCC Fig. AI.8 displays the winter months of ~~December - February, Figure ??~~ December–February, and AI.9 is for June–August. Figure 6 of this paper does not dis-

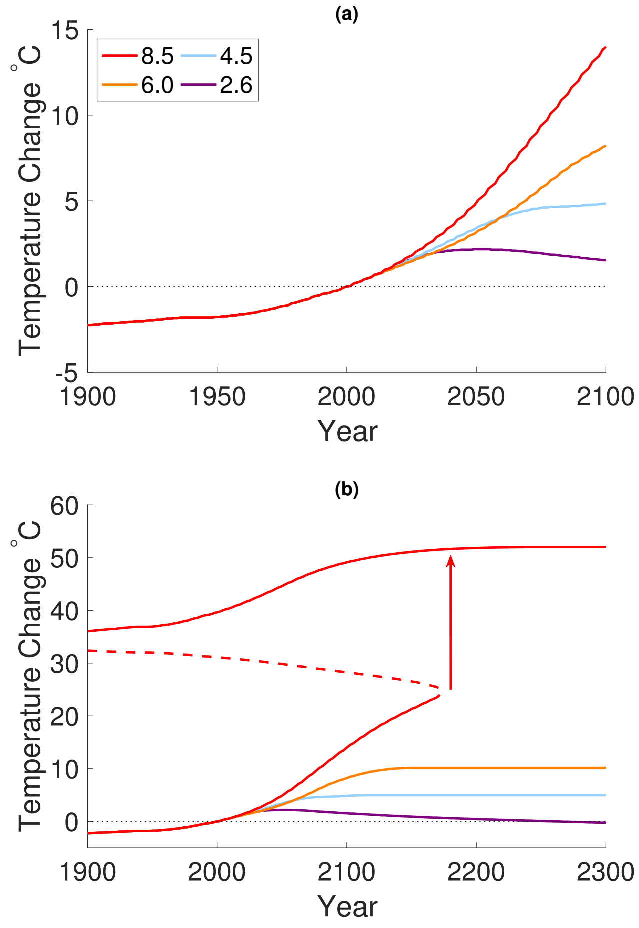

Figure 6. Arctic surface temperature change, relative to the year 2000 average temperature of -28.90°C, for each of the four RCP's with constant $F_O = 10\,\mathrm{W/m^2}$ and with $\delta = 0.6$. In (a), the EBM temperature change is projected to year 2100, and in (b) it is projected to year 2300, following the assumptions of the RCP pathways in Fig. 4. Note the dramatic jump in temperature on RCP 8.5, resulting from a saddlenode bifurcation, predicted near the year 2170. The vertical arrow is not an actual trajectory of the dynamical system, but rather represents the transition to a new equilibrium state, that occurs after the disappearance of the saddlenode.

tinguish surface covering, and is an annual average value. Figure~~AI.9 in (IPCC (2013)) also provides the sea and land surface temperature changes during the summer months of June - August.~~

~~Arctic surface temperature change, for each of the four RCP's with constant $F_O = 10\,\mathrm{W/m^2}$ and with $\delta = 0.6$. In **a)**, the temperature change is projected to year 2100, and in **b)** it is projected to year 2300, following the assumptions of the RCP pathways in Figure ??. Note the dramatic jump in temperature on RCP 8.5, resulting from a saddlenode bifurcation, predicted near the year 2160.~~

~~Figure ?? **a)** is in good agreement with the projections of (IPCC (2013))~~ 6 (a) shows predictions of the EBM to the year 2100, which is the same timeframe as for the IPCC GCM projections. Both use the RCP scenarios to determine hypothetical CO$_2$ concentrations (μ) by year, up to year 2100. Then both use these CO$_2$ concentrations as input to the respective models (EBM or GCM) to determine predicted climate changes for the same period. They are in good agreement, if a weighted average of the sea and land temperature changes are considered, and if the winter months are more representative of an annual value for the Arctic climate. ~~However, the projections in (IPCC (2013)) for Arctic region surface temperatures only extend to the year 2100. Figure ?? **b)** shows an extension of the EBM forecasts~~

Supported by the agreement until year 2100 between Fig. 6 (a) and the IPCC reported values of temperature change on the RCP paths, the EBM forecast was then extended to the year 2300, ~~with exactly~~ see Fig. 6 (b), which uses the same parameter values as ~~in Figure ?? **a)**~~Fig. 6 (a). It exhibits a ~~dramatic~~ saddlenode bifurcation for RCP 8.5 near the year ~~2160. This bifurcation causes~~ 2170. Following the disappearance of the cooler equilibrium state in this saddlenode bifurcation, bifurcation theory tells us that there exists a neighbourhood in the state space, where the saddlenode once existed, inside of which trajectories move slowly through a so-called “ghost equilibrium” that is a remnant of the saddlenode (the transit time has inverse square-root dependence on the unfolding parameter in that neighbourhood). Outside of that neighbourhood, trajectories evolve with velocity determined by c_S and c_A in Eq.s (1)(2), to the upper stable equilibrium point. (The vertical arrow in Fig. 6 (b) represents that transition, but is not an actual solution of the dynamical system, and similarly for the vertical arrows in Fig.s 7 and 10.) This bifurcation on RCP 8.5 results in a drastic increase in temperature: the mean Arctic temperature jumps by $+$~~27.8~~26.5°C, to the new value of $+$~~51.6~~22.5°C. ~~Although~~ This is warmer than the mean annual Arctic temperature in the Pliocene, but is consistent with what existed in the Eocene (Willard et al., 2019). Because of simplifications made in this EBM, these numbers should not be taken literally as ~~accurate forecasts because of simplifications in the EBM, the~~ quantitatively accurate forecasts; however, the qualitative existence of a dramatic increase in temperature due to a bifurcation must be taken seriously. The topological methods employed in this work ensure that bifurcation in this model is a mathematically persistent feature that will be manifest in all “nearby” models, see Kypke and Langford (2020).

The other three RCPs show no such jump in ~~Figure ??~~Fig. 6, and indeed all three stay well below freezing. However, it must be borne in mind that the IPCC assumptions (used here) have all four RCPs levelling off to a target value by the end of this century, see ~~Figure ??. This~~ Fig. 4. That may be overly optimistic.

3.2.2 Ocean and atmosphere heat transport feedback

In Figure ~~??~~6, the only forcing parameter that was changing was the CO$_2$ concentration (assumed due to anthropogenic forcing). Now we incorporate changes in ocean and atmosphere heat transport, which may amplify the effects of increasing CO$_2$ alone.

There is evidence that ocean heat transport F_O into the Arctic is increasing. For example, ~~(Koenigk and Brodeau (2014))~~ Koenigk and Brodeau (2014) project ocean heat transport above 70N to increase from 0.15 PW in 1860 to 0.2 and 0.3 PW in 2100, for RCP 2.6 and 8.5, respectively. At the same time, they find in their model that atmospheric heat transport decreases slightly, from 1.65 PW in 1850 to 1.6 PW (1.5 PW) for RCP 2.6 (RCP 8.5). These authors found that, in a stable climate state that ensures global energy conservation, F_O and F_A tend to be out of phase; see for example the coupled climate model in Koenigk and Brodeau (2014). However, Yang et al. (2016) show that in a more realistic situation when the climate is perturbed by both heat and freshwater fluxes, the changes in F_O and F_A may be in-phase. We assume the latter situation in this paper, see Fig. 7(b).

In our model, climate forcings F_O and F_A are expressed as power per unit area, W/m^2, determined as follows (see Table 2). First, the surface area of the Arctic region is estimated. The Arctic is taken to be the surface of the Earth above the 70th parallel; as such the surface area is

$$\text{Arctic Surface Area} = 2\pi R^2(1-\cos\theta), \tag{18}$$

where R is the radius of the Earth, 6371 km, and θ is 90° minus the latitude. Hence, the surface area of the Earth above 70° is approximately 1.538 $\times 10^{13}$ m^2. This leads to atmospheric and ocean heat fluxes into the Arctic as summarized in Table 2. Because the change in F_A is small relative to the changes in μ and F_O, F_A is kept constant at an intermediate value of 104 W/m^2 in ~~Figures ?? to ?? a)~~Fig.s 5 to 7(a).

~~Figure ?? a)~~

Figure 7(a) shows the change in Arctic surface temperature (relative to the year 2000 temperature of -28.90°C) for the four RCPs with the ocean heat flux F_O increasing linearly on each RCP until the year 2100, as projected in ~~(Koenigk and Brodeau (2014))~~Koenigk and Brodeau (2014), using their data for F_O in Table 2, ~~bur~~ but with constant $F_A = 104$. Beyond the year 2100, until 2300, the ocean heat transport F_O is held constant at its 2100 value. In this scenario, the onset of the jump (via a fold bifurcation) to a warm equable climate is advanced dramatically. The bifurcation for RCP 8.5 occurs in the year 2118, more than 40 years earlier than was the case with a constant F_O ~~(Figure ??)~~in Fig. 6. The temperatures

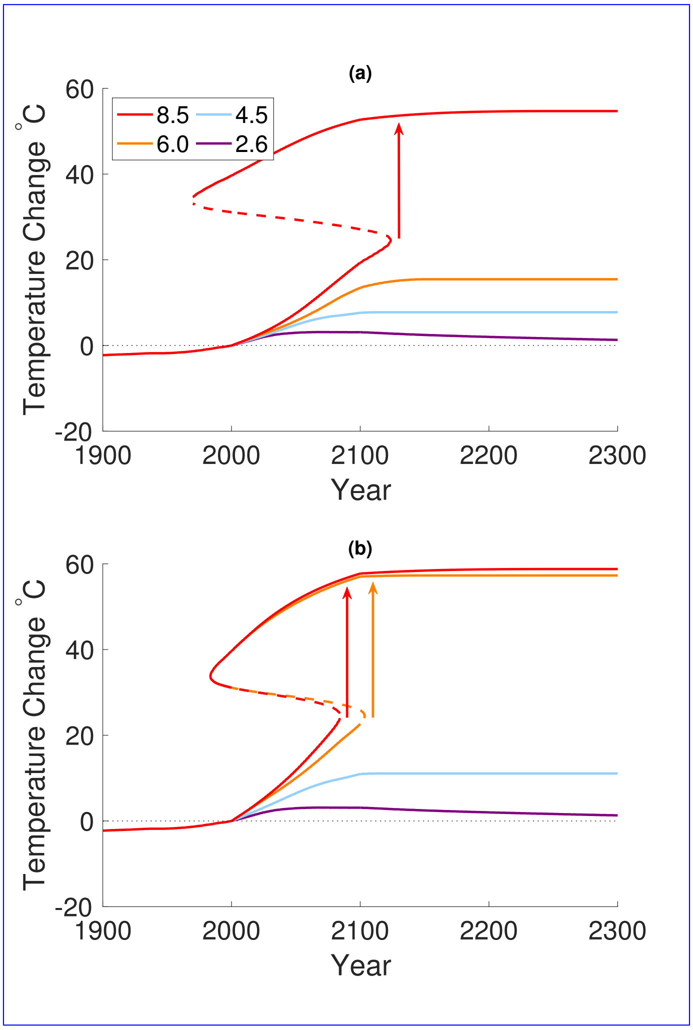

Figure 7. Arctic surface temperature change projected to year 2300 (relative to year 2000 temperature of -28.90°C), with linearly increasing ocean heat transport F_O, interpolating the data in ~~(Koenigk and Brodeau (2014))~~ Koenigk and Brodeau (2014), see Table 2. ~~a)~~ (a) With constant $F_A = 104$, the jump in temperature for RCP 8.5 now occurs nearly 40 years earlier than for the case of constant F_O shown in ~~Figure~~Fig. ~~??~~6. ~~b)~~ (b) The same as ~~a)~~ (a) except that in addition to increasing F_O, the atmosphere heat transport F_A also increases, as in Yang et al. (2016), linearly from 104 to 129 W/m^2. Now ~~, bifurcations~~ upward transitions occur on *both* RCP 8.5 and 6.0, ~~and they occur earlier than in a)~~as indicated by the arrows.

~~associated with the jump~~ before and after the jump in 2118 between two stable states are ~~from +23.8~~-4.6°C ~~in 2118 to~~ and +~~53.1~~24.7°C ~~in the year 2119~~respectively, a sudden increase of ~~29.9~~29.3°C. The other three RCPs remain below the freezing temperature.

Figure 7~~b)~~ (b) shows the same scenario as in ~~a)~~(a), with increasing μ and F_O, but with the atmospheric heat transport F_A also increasing~~linearly,~~ , linearly from 104 ~~to 129~~

W/m^2 in the year 2000 to 129 W/m^2 in 2100, and constant thereafter. In this case, ~~a bifurcation occurs not only for RCP 8.5, but also for RCP 6.0. Some authors have found that, in a stable climate state that ensures global energy conservation, F_O and F_A tend to be out of phase; that is, as F_O increases then F_A decreases; see for example the coupled climate model of (Koenigk and Brodeau (2014)). However, (Yang et al. (2016)) show that in a more realistic situation when the climate is perturbed by both heat and freshwater fluxes, the changes in F_O and F_A may be in-phase. We consider the in-phase case in Figure 7 **b)**, and find that it yields not only an earlier bifurcation~~ the saddlenode bifurcation occurs even earlier for RCP 8.5, ~~but also~~ and a new bifurcation appears for RCP 6.0~~, both of which~~. Both of these changes make mitigation more challenging.

3.2.3 Water vapour feedback

Overall, water vapour is known to be the most powerful greenhouse gas in the atmosphere ~~(Dai (2006); Pierrehumbert (2010); IPCC (2013))~~(Dai, 2006; Pierrehumbert, 2010; IPCC, 2013). Warming of the surface causes evaporation of more water vapour, which causes further greenhouse warming and a further rise in surface temperature. Thus, water vapour amplifies the warming due to other causes. This is called water vapour feedback. Empirical studies such as ~~(Dai (2006))~~ Dai (2006) show that the increase in surface specific humidity H with surface temperature T is close to that predicted by the Clausius-Clapeyron equation as in (6) (outside of desert regions). The relative humidity, RH or δ, changes little with surface temperature, even as the specific humidity H increases ~~(Serreze et al. (2012))~~(Serreze et al., 2012). For paleoclimates, ~~(Jahren and Sternberg (2003))~~ Jahren and Sternberg (2003) have described an Eocene Arctic rain forest with RH estimated to be $\delta = 0.67$. Modern data, from a variety of sources, suggest similar values of Arctic RH. For example, ~~(Shupe et al. (2011))~~ Shupe et al. (2011) report Arctic RH at the surface over 0.7 and atmospheric RH at 2.5 km altitude near 0.6, with relatively small seasonal and spatial variations.

Therefore, in the EBM (1)(2), it is assumed that the greenhouse warming effect of water vapour is determined by the Clausius-Clapeyron relation as in ~~equation~~ Eq. (6) and the RH δ remains constant. We assumed a value of $\delta = 0.60$ for the Arctic atmosphere in the previous section.

The Clausius-Clapeyron equation tells us that, below the freezing temperature ($\tau_S = 1$) the concentration of water vapour is very low and therefore it has very little greenhouse effect. However above freezing, if a source of water is available (e.g. ~~ocean~~oceans), then the concentration of water vapour and its greenhouse warming effect increase rapidly. This is shown clearly in ~~Figure ??~~Fig. 8, where the three curves show different levels of relative humidity δ, but all assume that CO$_2$ follows RPC 8.5. Here, the reference temperatures in year 2000 are as follows: Red curve −28.899°C, Green curve −29.418°C, Blue curve −30.320°C. On each of the curves of ~~Figure ??,~~ Fig. 8, the dashed portions with negative slope are unstable, while portions with positive slope are asymptotically stable (in the sense of Liapunov). Bistability (the coexistence of two stable solutions) occurs sooner when water vapour is present. The lower continuous blue curve with $\delta = 0$ shows no thawing ($\tau_S < 1$) in this range.

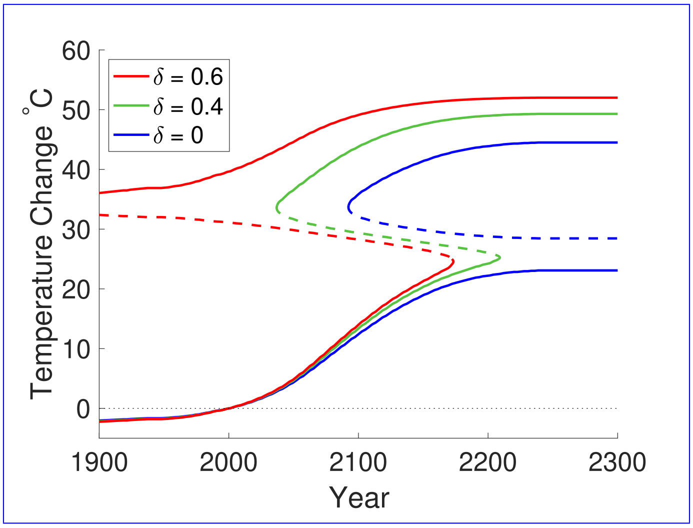

Figure 8. Arctic surface temperature change ~~, projected to year 2300 relative to year 2000,~~ with increasing relative humidity of water vapour, ~~$\delta = 0.0, 0.3, 0.6$~~$\delta = 0.0, 0.4, 0.6$, and with fixed ~~F_O, F_A~~F_O, F_A, projected to year 2300. (Temperature change is relative to the year 2000 temperature, see text.) On all three curves, CO$_2$ is increasing in time according to RCP 8.5. The red curve is essentially the same as that shown in ~~Figure~~Fig. ~~??~~ 6 with $\delta = 0.6$. The blue and green curves ~~are RCP 8.5, but with~~ have water vapour fixed at $\delta = 0.0$ and ~~$\delta = 0.3$~~$\delta = 0.4$, respectively. For temperatures significantly below freezing, water vapour makes little contribution to temperature change. However, above freezing ($\tau_S > 1$), the greenhouse warming effect of water vapour is dramatic.

3.2.4 Anthropocene Arctic EBM summary

This EBM for the Anthropocene Arctic predicts ~~a bifurcation producing~~ that a bifurcation will occur, leading to catastrophic warming of the Arctic, if CO$_2$ emissions continue to increase ~~unmitigated, even while~~ along RPC 8.5 without mitigation. This is true in the model even if ocean and atmosphere heat transport remain unchanged. The amplifying effects of ocean and atmosphere heat transport can make this abrupt climate change become even more dramatic, and occur even earlier. Water vapour feedback further intensifies global warming. However, the EBM predicts that RCP's with reduced CO$_2$ ~~mitigation strategies,~~ emissions (due for example to effective mitigation strategies if introduced soon enough~~,~~) may avert the drastic consequences of ~~this~~ such bifurcation.

Further work on Anthropocene Arctic climate modelling will include the effects of other positive feedback mechanisms, for example the greenhouse effects of the methane and CO$_2$ that will be released as the permafrost thaws in the Arctic, and the Hadley cell feedback that ~~will~~ may occur as global circulation patterns change. With such additional amplification in the Arctic taken into account, and no mitigation strategies in place, a saddlenode bifurcation ~~to a dramatically~~ resulting in a transition to a warmer Arctic climate state may ~~become even more likely~~occur even earlier than predicted by the present model.

3.3 EBM for the Anthropocene Antarctic

~~The Antarctic climate differs from the Arcticclimate in one major way: It~~ It has long been recognized that the climate of the Southern Hemisphere is generally colder than that of the Northern Hemisphere, for a number of reasons (Feulner et al., 2013). In particular the Antarctic is colder than the Arctic. The Antarctic climate is affected by the Antarctic Circumpolar Current (ACC), which flows freely west to east around Antarctica in the southern ocean, unimpeded by continental barriers. The ACC blocks the poleward heat transport from the warm oceans of the southern hemisphere ~~(Hartmann (2016))~~(Hartmann, 2016). Hence, F_O is restricted ~~between 0 and~~ to be below 20 W/m^2 in the Antarctic EBM. Additionally, the cold surface albedo $\alpha_C = 0.8$ is greater for the Antarctic than the Arctic, because the snow and ice that covers the continent is more pure than that in the Arctic. Cloud albedo is reduced, with a value of 7% as opposed to the value of 12.12% for the Arctic ~~(Pirazzini (2004))~~(Pirazzini, 2004). Atmospheric heat transport is ~~$F_A = 94$~~ $F_A = 97$ W/m^2, as determined in ~~(Zhang and Rossow (1997))~~Zhang and Rossow (1997). Finally, the Antarctic region is much drier than the Arctic, hence a relative humidity of $\delta = 0.4$ is used.

For the Antarctic, ~~Figure ??~~Fig. 9(a) is the equilibrium manifold for the energy balance model parameterized by (F_O, μ), and ~~Figure ??~~Fig. 9(b) is the projection of the fold bifurcations onto the parameter plane. In ~~Figure ??~~Fig. 9(b), the yellow area represents a warm stable climate, the blue area a cold stable climate, and the green area ~~the overlap~~ represents the overlap region (between the two fold bifurcations) where bistability exists. It can be seen in ~~Figure ??~~ Fig. 9 that a bifurcation from a cold state to a warm state in the EBM cannot occur for an ocean heat transport value of less than ~~$F_O = 2$~~ $F_O = 12$ W/m^2 and a carbon dioxide concentration less than $\mu = 3000$ ppm.

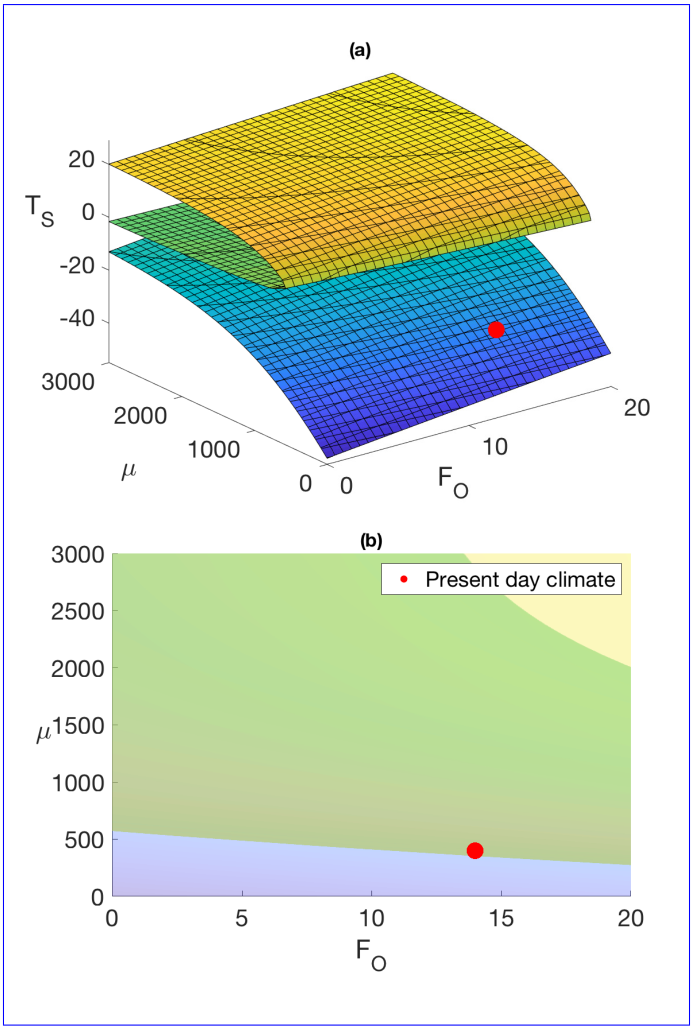

Figure 9. Energy Balance Model for the Antarctic. (a) 3D equilibrium manifold, (b) Projection of the fold bifurcations. The red dot locates today's climate conditions on the cold surface.

~~Figure?? shows the RCP curves for the Antarctic~~Figure 10(a) shows the temperature change, following each of the RCP curves in the Antarctic, extended to the year 2300. The reference temperature is −32.78°C, for the year 2000, and the value of ocean heat transport into the Antarctic is assumed to be $F_O = 14$ W/m^2, an annual mean for the sea-ice zone (approximately 70°S) of the Antarctic, as determined in ~~(Wu et al. (2001))~~Wu et al. (2001). This scenario does not exhibit a bifurcation from a cold climate state to a warm state. This suggests that for the Antarctic, a change in μ alone is not sufficient to cause a hysteresis loop to exist, between ~~the two possible~~ two coexisting stable states, in the context of modern and near-future carbon dioxide concentrations.

Figure~~??~~ 10(b) presents the Antarctic model for values of F_O that increase with time as μ ~~does~~increases. The value of F_O is kept constant at 5 W/m^2 until the year 2000, after which ~~point~~ time it increases linearly up to the year 2100, where it has a value of $F_O = 20$ W/m^2, after which it is held constant again. This increase might represent an increase in sea levels, caused by thawing of the

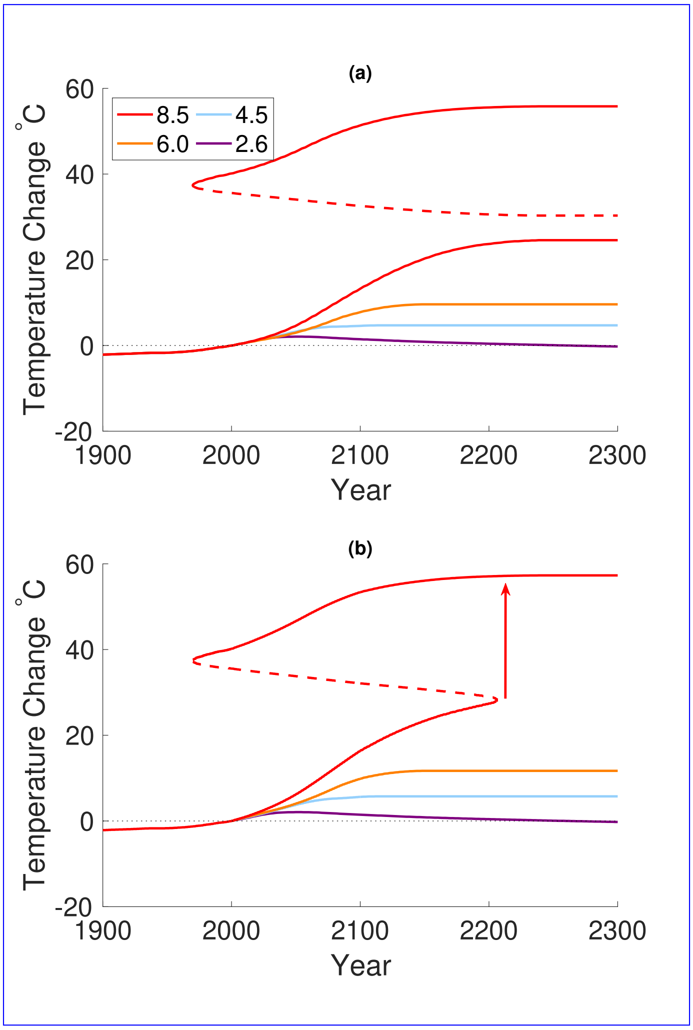

Figure 10. Antarctic surface temperature change projected to year 2300, relative to year 2000 ~~,~~ temperature of −32.78°C; (a) on each ~~RCP. Constant~~ of the four RCPs, with constant $F_O = 14$ W/m^2; (b) on RCPs 8.5 and 2.6, together with increasing ocean heat transport F_O, see text for details. The upward arrow indicates the transition to a warmer equilibrium climate state, after the saddlenode bifurcation.

Arctic, loss of the Antarctic ice shelves, and subsequent increase in ocean heat transport ~~(Koenigk and Brodeau (2014))~~(Koenigk and Brodeau, 2014). The first thing to notice is ~~a that~~ that a hysteresis loop now exists. With increasing CO$_2$ on RCP 8.5, there is a a jump between stable states, from ~~+29.1°C in 2224 to +56.5 °Cin the year 2225.~~ $\Delta T = +29.1$°C to $\Delta T = +56.5$°C, occurring in year 2225, where ΔT is the change in surface temperature relative to the year 2000 temperature of −32.78°C. The above-freezing average temperatures on the upper warm branch of equilibrium states are consistent with estimates of Antarctic temperatures in the Eocene (Passchier et al., 2013). Such a transition would imply melting of the Antarctic ice cap and a drastic rise in sea levels around the world. The return bifurcation ~~,~~ from warm to cold ~~, may be seen in Figure ??, but would be difficult to achieve~~(with time reversed), is visible in Fig. 10(b). The “cold-to-warm” ~~bifurcation~~ transition occurs at a later time in the Antarctic than in the Arctic, and at a ~~greater~~ higher temperature. The ~~difference in the Antarctic bifurcations, as compared to the Arctic, is~~ differences between the Antarctic and Arctic bifurcations in the EBM are due to the ~~difference~~ differences in ocean heat transport and ice albedos. The difference could be larger if other factors are taken into account, for example that the Antarctic has thicker ice, hence more heat is required to melt enough ice to cause a change in albedo. This could be represented with a ~~different value in~~ larger value of ω ~~: a smaller value for~~ in the $\tanh$ switch function~~smoothness represents~~; then a greater temperature change is required for the function to switch from a cold albedo value to a warm one.

~~Antarctic surface temperature change projection to year 2300 relative to year 2000 with increasing F_O, see text.~~

3.4 EBM for the Anthropocene Tropics

Next, the EBM is adapted to model the climate of the Tropics by choosing parameter values ~~which~~ that are annual mean, zonally averaged values at the equator. This gives insolation $Q = 418.8$ W/m^2 and relative humidity $\delta = 0.8$. Heat transports $F_A = -38$ W/m^2 and $F_O = -39$ W/m^2 are both negative, because heat is transported away from the equator towards the poles ~~(Hartmann (2016))~~(Hartmann, 2016). The shortwave cloud cooling ~~, i.e.~~ ξ_R (the albedo of the clouds), is also greater in the Tropics, and the surface has a lower albedo. The value ~~used~~ $\xi_R = 22.35\%$ is determined in the Appendix from the global energy budgets of ~~(Trenberth et al. (2009); Wild et al. (2013)), a value of 22.35%~~Trenberth et al. (2009); Wild et al. (2013).

As the Tropics have annual average temperatures well above the freezing point of water, ice-albedo feedback is absent in the Tropics and a bifurcation from a cold stable state to a warm state can not occur under Anthropocene conditions. However, if forced to low F_O, F_A values and very low carbon dioxide levels, the climate state known as “snowball Earth" ~~(Pierrehumbert (2010))~~ (Kaper and Engler, 2013; Pierrehumbert, 2010) is a possibility. That scenario is not explored in this paper, as it is not relevant to the Anthropocene.

The large relative humidity of $\delta = 0.8$ in the tropics serves to mitigate the radiative forcing of increasing CO$_2$. Water vapour is a much more effective greenhouse gas than carbon dioxide ~~, so for a climate that~~ (Pierrehumbert, 2010). The atmosphere of the Tropics contains more water vapour (the product of greater relative humidity and warmer temperatures)~~, the effect of an increase in carbon dioxide is smaller compared to the case of a climate where water vapour is~~

~~less abundant (Pierrehumbert (2010))~~. The total atmospheric longwave absorption η is ~~as given in equation~~ given in Eq. (9)~~; so in a region where~~. In the EBM of the Tropics, the water vapour content is ~~high,~~ so high, that η_W (and thus total absorptivity η) ~~will be~~ is almost "maxed out" at ~~1.~~ $\eta \approx 1$. Hence the total absorptivity is dominated by the contribution due to water vapour, and an increase in CO_2 concentration ~~will have~~ has little additional greenhouse warming effect.

~~Figure ??~~ Figure 11 reveals relatively low increases in temperature for the Tropics compared to the Poles, as CO_2 concentration increases along the RCPs. Both the absence of a bifurcation, and the mitigation due to a large existing water vapour greenhouse forcing, taken together cause the temperature increase relative to the year 2000 to be less than 2°C, in all four RCP scenarios.

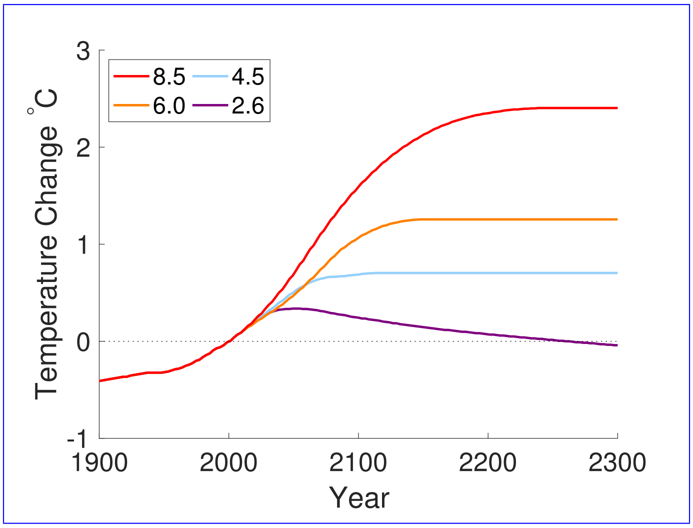

Figure 11. Tropical surface temperature changes ~~,~~ for the four RCP scenarios~~. Forecast~~, forecast to year 2300 ~~,~~ relative to year 2000 (25.19°C), with constant F_O and F_A. The temperature change is ~~limited~~ relatively small in the Tropics.

3.5 EBM for ~~Globally Averaged Temperature~~globally averaged temperature

Changes in globally averaged temperature can be modelled more easily than changes in regional temperatures, due to the fact that, in a globally averaged equilibrium model, overall net horizontal transport of energy, by the oceans and the atmosphere, are both zero. Thus, the two-layer EBM (4) (5), globally averaged with $F_O = 0$ and $F_A = 0$, ~~becomes~~ is simplified as follows.

$$\frac{d\tau_S}{d\hat{s}} = (1-\alpha)(1-\xi_A-\xi_R)q - f_C + \beta i_A - \tau_S^4 \tag{19a}$$

$$\frac{di_A}{d\hat{s}} = \chi[f_C + q\xi_A + \eta\tau_s^4 - i_A]. \tag{19b}$$

Here α is as defined in ~~equation~~ Eq. (8), η is as in (9) and f_C is as in (10). Parameters ~~ξ_A, ξ_{CI}~~ ξ_A, ξ_R are as in Table 1 and Section 2.1.

~~Figure ?? shows the~~ Figure 12 shows the change in globally averaged equilibrium surface temperature, relative to the year 2000 global average ($\tau_S = 1.064$, 17.59°C), as determined by the EBM (19) ~~as a function of time, under the assumption~~ to the year 2300. It is assumed that CO_2 evolves with time along each of the four RCPs defined in ~~(IPCC (2013))~~ IPCC (2013) and displayed in ~~Figure ??~~Fig. 4. The other parameters, assumed constant, are as follows. The global relative humidity δ is fixed at a value of 0.74. This is determined from ~~(Dai (2006))~~Dai (2006), where it lies at the lower end of a range of averages. Surface albedo is highly variable regionally, so a global average was calculated from ~~(Wild et al. (2013))~~Wild et al. (2013), much like the atmospheric shortwave absorption and the cloud albedo. From ~~Figure~~ Fig. 1 of ~~(Wild et al. (2013))~~Wild et al. (2013), of the global average solar radiation of 185 W/m^2 that reaches the surface, a portion 24 W/m^2 is reflected. Thus, the global average surface albedo is $\frac{24}{185} = 0.13 = 13\%$. The values for cloud albedo and atmospheric shortwave radiation are calculated as follows. The global average incident solar radiation Q at the top of the atmosphere is 340 W/m^2, of which $\frac{100-24}{340} = 0.2235 = 22.35\%$ is reflected by clouds, and $\frac{79}{340} = 0.2324 = 23.24\%$ is absorbed by the atmosphere. The Planetary Boundary Layer (PBL) altitude is ~~700 m (Ganeshan and Wu (2016))~~600 m (Ganeshan and Wu, 2016). Finally, ~~the wind speed U,~~ for the purposes of sensible and latent heat transport ~~, is 6~~ (see Appendix), the wind speed U is 5 m/s ~~(Nugent et al. (2014))~~(Nugent et al., 2014) and the drag coefficient is $C_D = 1.5 \times 10^{-3}$.

~~The 1980–1999 global average temperature for this model was calculated to be $\tau_S = 1.062$ (equivalently 15.84°C or 290 K), using the data displayed in Figure ??. This is approximately equal to the global average value 289 K determined from the data in (Wild et al. (2013)), for the period 2001–2010. The changes in surface temperature from this reference value, as shown in Figure ??, agree well with the values predicted in the IPCC report; namely, 7.8°C for RCP 8.5, 2.5°C for RCP 4.5, and 0.6°C for RCP 2.6 IPCC (2013). (A value for RCP 6.0 was not given in (IPCC (2013)).)~~

3.6 Equilibrium ~~Climate Sensitivity~~climate sensitivity

Equilibrium climate sensitivity (ECS) is a useful and widely-adopted tool used to estimate the effects of anthropogenic forcing in a given climate model. The ECS of a model is defined as the change in the globally averaged surface temperature, after equilibrium is obtained, in response to a doubling of atmospheric CO_2 levels ~~(IPCC (2013); Knutti et al. (2017); Priostosescu and Huybers (2017))~~(IPCC, 2013; Knutti et al., 2017; Priostosescu and Huybers, 2017)

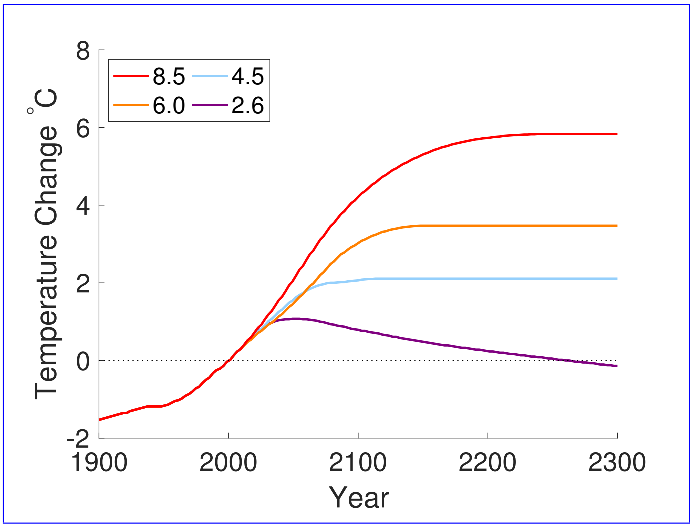

Figure 12. ~~Globally~~ Change in globally averaged surface temperature, relative to year 2000 global average temperature of 17.59 °C, calculated to the year 2300 for the EBM on each of the four RCPs. ~~Change in globally averaged surface temperature, relative to 1980-1999 average, for each of the four RCPs.~~

. The starting carbon dioxide concentration is that of the preindustrial climate, taken to be $\mu = 270$ ppm. The doubled value is then $\mu = 540$ ppm. Since the Earth has not yet experienced a doubling of CO_2 concentration since the industrial revolution, these numbers cannot be verified. Calculation of the global ECS for the EBM of this paper facilitates comparisons with other climate models as reported in ~~(IPCC (2013))~~IPCC (2013).

3.6.1 ECS for the globally averaged EBM

Table 3 gives both the non-dimensional τ_S and the degree Celsius temperature values for the $\mu = 270$ climate, the $\mu = 540$ climate, and the temperature difference. This difference is the ECS of the global EBM of this paper.

For the models used in ~~(IPCC (2013))~~IPCC (2013), ECS values lie within a *likely* range of 1.5 °C to 4.5 °C. Values of less than 1 °C are deemed to be *extremely unlikely*, and greater than 6 °C are *very unlikely* ~~(IPCC (2013))~~(IPCC, 2013). The value of ~~4.55~~ 4.343 °C calculated for this global EBM lies just ~~above~~ inside the *likely* range, ~~but is still well below the *very unlikely* boundary~~at the high end. Recent work gives evidence that statistical climate models based on historical data tend to lie on the lower end of *likely* ECS values, with a range of 1.5 °C to 3 °C, whereas nonlinear GCMs tend to have larger ECS values ~~(Priostosescu and Huybers (2017))~~(Priostosescu and Huybers, 2017). Therefore, as the global EBM presented in this paper is nonlinear and is based on ~~geophysics~~ physical rather than statistical ~~data~~modelling, it may be expected to fall on the side of larger ECS values.

3.6.2 Regional ECS values

Local ECS values may be determined for each of the three regional models, ~~for~~ the Arctic, Antarctic and Tropics, as defined in Sections 3.2 to 3.4. These values are given in Table 4. In all cases, F_O values are kept constant at their minimal values: 10 W/m^2 for the Arctic, 14 W/m^2 for the Antarctic, and -39 W/m^2 for the tropics. The regional ECS values are high, ~~8.0 and 7.5~~ 7.95 and 7.54 °C respectively, for the Arctic and Antarctic, and low, ~~1.1~~ 1.27 °C for the Tropics. Although the Earth has not yet experienced a doubling of CO_2 concentrations since the industrial revolution, these ECS values are consistent with observations to date.

4 Conclusions and future work

The analysis of this paper ~~presents a mathematical proof that a~~ shows that a cusp bifurcation can occur in an energy balance model (EBM)~~for~~, which could lead to hysteresis behaviour and an abrupt warming of the anthropocene climate, ~~which~~ to a climate state that is like nothing that has existed on Earth since the Pliocene. The model has been constructed from ~~the~~ fundamental nonlinear processes of atmospheric physics. This bifurcation is most likely to occur in the Arctic climate. It would lead to catastrophic warming~~in the climate system~~, if increases in atmospheric CO_2 continue on their current pathway. However, if the increase in atmospheric CO_2 is mitigated sufficiently, this bifurcation ~~, causing catastrophic climate change,~~ can still be avoided. Climate changes in the Arctic, Antarctic and Tropics are compared. The globally averaged equilibrium climate sensitivity (ECS) of the EBM is ~~shown to be~~ 4.34°C, which is at the high end of the ~~range considered in (IPCC (2013))~~likely range reported in IPCC (2013).

Future work will strengthen the conclusions of this paper by extending this simple EBM to more comprehensive ~~Earth system~~ models, which still allow rigorous bifurcation analysis to be performed. In the first generalization, the two-layer model will be replaced with a column model, with the atmosphere extending continuously from the surface to the tropopause. The ICAO International Standard Atmosphere assumption will be replaced with a Schwarzschild radiation model of the atmosphere (Pierrehumbert, 2010), which will determine the lapse rate from the solution of a two-point boundary value problem. This Schwarzschild column model will be used to study, in addition to the positive feedback processes of this paper, the amplifying effects of methane from permafrost feedback in the Arctic.

The next generalization will ~~be to~~ combine the ideas of these energy balance models with a 3D ~~model, with~~ Navier-Stokes-Boussinesq ~~PDEs representing the convective atmosphere in a~~ PDE model, representing the convectively driven atmosphere as a fluid in a rotating spherical shell, ~~as presented in~~

~~(Lewis and Langford (2008); Langford and Lewis (2009)), but with the addition~~ presented in Lewis and Langford (2008); Langford and Lewis (2009). In that model, surface temperatures were prescribed as boundary conditions; however, with the assumption of an energy balance constraint~~like that in the Schwarzschild column model, which will determine implicitly the surface temperature. The relationship between polar amplification and Hadley cell expansion will be explored with this model.~~, the meridional surface temperature gradient will be determined implicitly. Meridional heat transport also will be determined in this model, and may be compared with the poleward heat transports in the EBM of this paper. The code to solve this PDE model for a cusp bifurcation has been written. Later, guided by these results, the climate bifurcations found in these analytical models will be sought in an open source General Circulation Model. This hierarchy of models is expected to add credibility to the prediction, presented here, that the Earth's climate system ~~may exhibit~~ is capable of exhibiting dramatic topological changes (bifurcations) in the Anthropocene, leading to a climate state that resembles the pre-Pliocene climate of Earth.

Appendix. Determination of ~~Parameter Values~~ parameters in the Anthropocene EBM

The determination of the physical parameters appearing in the EBM (4)(5) is summarized here. In most cases, these parameters were determined in earlier papers of the authors ~~(Dortmans et al. (2019); Kypke and Langford (2020)). The starting~~ dealing with paleoclimates (Dortmans et al., 2019; Kypke and Langford, 2020). The focal point is the scaled, two-dimensional ~~equations~~ Eq.s (4)(5) in Section 2.1, with α given by (8)~~and~~, η given by (9) and f_C given by (10).

First consider the incoming solar radiation Q. A fraction ξ_A is absorbed by the atmosphere and a fraction ξ_R is reflected by the clouds, as seen in ~~Figure ?? and equations~~ Fig. 1 and Eq.s (4)(5). These fractions were determined in ~~(Kypke (2019))~~ Kypke (2019) and Appendix A1 of ~~(Dortmans et al. (2019))~~Dortmans et al. (2019), using data for the global average energy budget described in ~~(Trenberth et al. (2009); Wild et al. (2013); Kim and Ramanathan (2012))~~Trenberth et al. (2009); Wild et al. (2013); Kim and Ramanathan (2012). The globally averaged values were $\xi_A = 0.2324$ and $\xi_R = 0.2235$ as listed in Table 1. For the polar regions, the albedo of clouds is less than elsewhere. Using data collected in the Surface Heat Budget of the Arctic (SHEBA) program ~~(Intrieri et al, (2002); Shupe and Intrieri (2003)), the~~ (Intrieri et al., 2002; Shupe and Intrieri, 2003), the revised polar value of $\xi_R = 0.1212$ was determined in ~~(Kypke (2019))~~Kypke (2019).

Clouds in the atmosphere have a second main effect, the absorption of a fraction η_{Cl} of the longwave radiation outgoing from the surface of the Earth ~~(Hartmann (2016))~~(Hartmann, 2016). This effect warms the Earth's atmosphere. Through data in the SHEBA program, the longwave cloud forcing in the Arctic was found to be 51 W/m^2 in the paper ~~(Shupe and Intrieri (2003))~~of Shupe and Intrieri (2003). Using this SHEBA data, ~~Kypke (2019)~~ Kypke (2019) determined the fraction $\eta_{Cl} = 0.255$, as used in (9), see Table 1.

The absorption coefficients k_C for carbon dioxide and k_W for water vapour in the atmosphere (see Table 1), were calculated using an empirical approach, based on the modern-day global energy budget ~~(Trenberth et al. (2009); Wild et al. (2013))~~(Trenberth et al., 2009; Wild et al., 2013). Figure 1 in ~~(Trenberth et al. (2009))~~ Trenberth et al. (2009) provides the global mean surface radiation as 396 W/m^2, along with an atmospheric window of 40 W/m^2. This atmospheric window, $\frac{40}{396} \approx 0.1$, is then equal to $1 - \eta$. ~~(Schmidt et al. (2010))~~ Schmidt et al. (2010) provide percentage contributions of carbon dioxide and water vapour and clouds in an all-sky scenario, based on simulations using modern climate conditions from the year 1980. The calculated values for η_C and η_W are then used to calculate the corresponding optical depths λ_C and λ_W for the case of the modern atmosphere, and these are used to solve for k_C and k_W, which then appear in the G_C and G_{W2} terms respectively, in Table 1 and ~~Equation~~ Eq. (7).

The vertical transport of sensible and latent heat is a difficult and complicated process to model, so many approximations are made to keep it within the scope of this work. For more details, see ~~(Kypke (2019))~~Kypke (2019). The heat transports are modelled via *bulk aerodynamic exchange* formulae describing fluxes between the surface and the atmosphere ~~as described in (Pierrehumbert (2010); Hartmann (2016))~~(Pierrehumbert, 2010; Hartmann, 2016). For the sensible heat flux, c_p is the specific heat of the air being heated, and T is its temperature. The bulk aerodynamic formula for sensible heat (SH) is

$$SH = c_p \, \rho \, C_{DS} \, U(T_S - T_A), \tag{20}$$

where C_{DS} is the drag coefficient for temperature and U is the mean horizontal wind velocity. The density of the atmosphere ρ is determined as a function of both surface temperature T_S and altitude Z using the barometric formula, and a constant lapse rate Γ ~~(ICAO (1993))~~ (ICAO, 1993) is used to determine the temperature gradient.

In the case of latent heat (LH), the moisture content is represented by $L_v r$, where L_v is the latent heat of vaporization of water and r is the *mass mixing ratio* of condensable air to dry air ~~(Pierrehumbert (2010)),~~ (Pierrehumbert, 2010). Then

$$LH = L_v \, \rho \, C_{DL} \, U(r_S - r_A), \tag{21}$$

where C_{DL} is the drag coefficient for moisture. In the following, for simplicity, we set

$$C_{DS} = C_{DL} \equiv C_D.$$

The mass mixing ratio is equal to the saturation mixing ratio times the relative humidity. The saturation mixing ratio depends on the saturation vapour pressure, which is a function of temperature as given by the Clausius-Clapeyron ~~equation~~ Eq. (6). The sensible and latent heat transports are combined into a single term, F_C, which replaces the F_C term that was introduced in ~~Figure ?? and Section 2~~Dortmans et al. (2019). This term is defined here as a function of surface temperature T_S,

$$F_C(T_S) = \frac{C_D U}{(T_S - \Gamma Z)}\left[\frac{c_p P_0 \Gamma Z}{R_A} + \frac{L_v P^{sat}(T_R)}{R_w}\left(e^{\left[G_{W1}\frac{T_S - T_R}{T_S}\right]} - \delta e^{\left[G_{W1}\frac{T_S - \Gamma Z - T_R}{T_S - \Gamma Z}\right]}\right)\right] \qquad (22)$$

Here, P_0 is the atmospheric pressure at the surface $(Z = 0)$ and R_A is the ideal gas constant specific to dry air. This equation is scaled by $\frac{1}{\sigma T_R^4}$ to nondimensionalize it, creating $f_C = \frac{F_C}{\sigma T_R^4}$ in (10), where $T_R = 273.15$ K is the reference temperature. As this f_C represents energy moving from the surface to the atmosphere, it is subtracted from the surface ~~equation~~ Eq. (4) and added to the atmosphere ~~equation~~ Eq. (5). A different model of F_C, used by the authors in ~~(Dortmans et al. (2019))~~Dortmans et al. (2019), was a simple functional form calibrated to empirical data. The result was a relationship between F_C and T_S that is quantitatively very similar to that given by ~~. In (Kypke and Langford (2020)~~ ~~)~~(22). In Kypke and Langford (2020), F_C was set equal to zero for the paleoclimate Arctic and Antarctic models for simplicity, since both SH and LH are very small for ~~below freezing temperatures~~temperatures that are below freezing.

Acknowledgements

The authors gratefully acknowledge financial support of the Natural Sciences and Engineering Research Council of Canada and thank ~~M. Garvie for generous assistance~~the two referees for suggestions and constructive criticisms that have improved this paper.

Code/~~Data~~ data availability

~~There are no supplemental Code or Data files~~The MATLAB files, used to solve the model equations and to produce the figures in this article, have been posted online at https://doi.org/10.5281/zenodo.3834344 (Kypke et al., 2020).

Author contributions

The original conception of this ~~work~~ research project was due to W. Langford. Most of the mathematical analysis and computations were performed by K. Kypke, ~~in~~ starting with his M.Sc. Thesis ~~(Kypke (2019))~~(Kypke, 2019). A. Willms co-supervised the ~~work~~ thesis and provided valuable ~~insights~~contributions and insights throughout the course of the work.

Competing interests

The authors declare no competing interests.

References

Alley, R. B., Marotzke, J., Nordhaus, W. D., Overpeck, J. T., Peteet, D. M., Pielke Jr., A., Pierrehumbert, R. T., Rhines, P. B., Stocker, T. F., Talley, L. D., and Wallace, J. M.~~2003“~~: Abrupt climate change~~”~~, Science 299, 2005–2010~~.~~, 2003.

Ashwin, P., Wieczorek, S., Vitolo, R. and Cox, P.: Tipping points in open systems: bifurcation, noise-induced and rate-dependent examples in the climate system, Phil. Trans. Roy. Soc. A 370, 1166–1184, 2012.

Barnosky, A.D., Hadly, E. A., Bascompte, J., Berlow, E. L., Brown, J. H., Fortelius, M., Getz, W. M., Harte, J., Hastings, A., Marquet, P. A., Martinez, N. D., Mooers, A., Roopnarine, P., Vermeij, G., Williams, J. W., Gillespie, R., Kitzes, J., Marshall, C., Matzke, N., Mindell, D. P., Revilla, E. and Smith, A. B.~~2012“~~: Approaching a state shift in Earth's biosphere~~”~~, Nature 486, 52–58~~.~~, 2012.

Barron, E.J., Thompson, S.L. and Schneider, S.H.~~1981“~~: An ice-free Cretaceous? Results from climate model simulations, ~~”~~Science 212, 10–13~~.~~, 1981.

Bathiany, S., Dijkstra, H., Crucifix, M., Dakos, V., Brovkin, V., Williamson, M.S., Lenton, T.M. and Scheffer, M.~~2016“~~: Beyond bifurcation: using complex models to understand and predict abrupt climate change~~”~~, Dyn. Stat. Clim. ~~System~~ Syst. 2016, doi:10.1093/climsys/dzw004.

Björk, G., Stranne, C. and Borenäs, K.~~2013“~~: The sensitivity of the Arctic Ocean sea ice thickness and its dependence on the surface albedo parameterization~~”~~, J. ~~Climate~~ Clim. 26, 1355–1370~~.~~, 2013.

Brovkin, V., Claussen, M., Petoukhov, V. and Ganopolski, A.: On the stability of the atmosphere-vegetation system in the Sahara/Sahel region. J. Geophys. Res. 103, D24, 31,613–31,624, 1998.

Budyko, M. I.~~1968“~~: The effects of solar radiation variations on the climate of the Earth~~”~~, Tellus 21, 611–619~~.~~, 1968.

Dai, A.~~2006“~~: Recent climatology, variability and trends in global surface humidity~~”~~, J. ~~Climate~~ Clim. 19, 3589–3606~~.~~, 2006.

Dijkstra, H. A.~~2013~~: Nonlinear Climate Dynamics, Cambridge University Press, New York~~.~~, 2013.

Dijkstra, H. A.: Numerical bifurcation methods applied to climate models: analysis beyond simulation, Nonlin. Processes Geophys. 26, 359–369, 2019.

Ditlevsen, P. D. and Johnsen, S. J.~~2010“~~: Tipping points: Early warning and wishful thinking~~”~~, Geophys. Res. Lett. 37, 2010. L19703, doi:10.1029/2010GL044486.

Dortmans, B., Langford, W. F., and Willms, A. R.~~2018“A Conceptual Model~~ : A conceptual model for the Pliocene ~~Paradox”~~paradox, in *Recent Advances in Mathematical and Statistical Methods*, Springer Proceedings in Mathematics and Statistics V. 259, eds. Kilgour, D. M., Kunze, H., Makarov, R., Melnik, R. and Wang, X., IV AMMCS International Conference, Waterloo, Canada, August 20–25, 2017, Springer Nature Switzerland AG. pp. 339–349~~.~~, 2019.

Dortmans, B., Langford, W. F., and Willms, A. R.~~2019“An Energy Balance Model for Paleoclimate Transitions”~~: An energy balance model for paleoclimate transitions, Clim. Past 15, 493–520~~.~~, 2019. doi.org/10.5194/cp-15-493-2019.

Drijfhout, S., Bathiany, S., Beaulieu, C., Brovkin, V., Claussend, M., Huntingford, C., Scheffer, M., Giovanni Sgubin, G. and Swingedouw, D.~~2015“~~: Catalogue of abrupt shifts in Intergovernmental Panel on Climate Change climate models~~”~~, PNAS doi/10.1073/pnas.1511451112~~.~~, 2015.

Feulner, G., Rahmstorf, S., Levermann, A. and Volkwardt, S.: On the origin of the surface air temperature difference between the hemispheres in Earth's present-day climate, J. Clim. 26, 7136–7150, 2013.

Ganeshan, M. and Wu, D. L.~~2016“~~: The open-ocean sensible heat flux and its significance for Arctic boundary layer mixing during early fall~~”~~, Atmosph. Chem. Phys. 16, 13173–13184~~.~~, 2016.

Ghil, M.: Hilbert problems for the geosciences in the 21st century, Nonlinear Processes Geophys. 8, 211–222, 2001.

Ghil, M. and Lucarini, V.: The Physics of Climate Variability and Climate Change, arXiv 1910.00583v2, 26 Feb 2020.

Hartmann, D.L.~~2016~~: Global Physical Climatology, Second Edition. Elsevier, Amsterdam~~.~~, 2016.

International Institute for Applied Systems Analysis (IIASA). The Representative Concentration Pathways data for ~~Figure ??~~ Fig. 4 were downloaded from http://www.iiasa.ac.at/web-apps/tnt/RcpDb/dsd? in 2019.

Intergovernmental Panel on Climate Change: Climate Change 2013: The Physical Science Basis. In: Contribution of Working Group I to the Fifth Assessment Report of the Intergovernmental Panel on Climate Change, edited by: Stocker, T. F., Qin, D., Plattner, G. K., Tignor, M., Allen, S. K., Boschung, J., Nauels, A., Xia, Y., Bex, V., and Midgley, P. M.~~2013~~: Cambridge Univ. Press, Cambridge, UK and New York, NY, USA, 2013. available at: http://www.ipcc.ch/ (last access: 11 March 2019).

International Civil Aviation Organization~~. 1993~~: Manual of the ICAO Standard Atmosphere: extended to 80 kilometres. Third Edition. ICAO, 1000 Sherbrooke Street West Suite 400, Montreal, Quebec, Canada H3A 2R2, 1993.

Intrieri, J. M., Fairall, C. W., Shupe, M. D., Persson, P. O. G., Andreas, E. L., Guest, P. S. and R. E. Moritz, R. E.~~2002“~~: An annual cycle of Arctic surface cloud forcing at SHEBA~~”~~. J. Geophys. Res. 107, 13–14~~.~~, 2002.

Jahren, A. H. and Sternberg, L. S. L.~~2003“~~: Humidity estimate for the middle Eocene Arctic rain forest~~”~~, Geology 31, 463–466~~.~~, 2003.

Kaper, H. and Engler, H.~~2013~~: Mathematics and Climate, Society for Industrial and Applied Mathematics, Philadelphia~~.~~, 2013.

Kim, D. and Ramanathan, V.~~2012“~~: Improved estimates and understanding of global albedo and atmospheric solar absorption~~”~~, Geophys. Res. Lett. 39, 2012. L24704.

Knutti, R., Rugenstein, M. A. A., and Hegerl, G. C.~~2017“~~: Beyond equilibrium climate sensitivity~~”~~. Nature Geosci. 10, 727–744~~.~~, 2017.

Koenigk, T. and Brodeau, L.~~2014“~~: Ocean heat transport into the Arctic in the twentieth and twenty-first century in EC-Earth~~”.~~ ~~Climate Dynamics~~ . Clim. Dyn. 42, 3101–3120~~.~~, 2014.

Kuznetsov, Yuri A.~~2004*Elements of Applied Bifurcation Theory, Third Edition.*~~ : Elements of Applied Bifurcation Theory, Third Edition. Applied Mathematical Sciences Vol. ~~112.~~ 112, Springer-Verlag, New York~~.~~, 2004.

Kypke, K. L.~~2019~~: Topological Climate Change and Anthropogenic Forcing. M.Sc. Thesis, Department of Mathematics and Statistics, University of Guelph~~.~~, Guelph, Ontario, Canada~~.~~, 137 pp., 2019.

Kypke, K. L. and Langford, W. F.~~2020“~~: Topological climate change~~”, to appear in International Journal of Bifurcation and Chaos, V. 20~~, Int. J. Bifurcation Chaos, 30, No. ~~2.~~ 2, 29 pp., 2020. DOI: 10.1142/S0218127420300050

Kypke, K. L., Langford, W. F. and Willms, A. R.: MATLAB files for figures for “Anthropocene Climate Change” in Nonlinear Processes in Geophysics, 2020. Zenodo DOI: 10.5281/zenodo.3834344 posted 2020 May 19, URL: https://doi.org/10.5281/zenodo.3834344

Langford, W.F. and Lewis, G.M.~~2009“~~: Poleward expansion of Hadley cells~~”~~, Can. Appl. Math. Quart. 17, 105–119~~.~~, 2009.

Lenton, T. M., Held, H., Kriegler, E., Hall, J. W., Lucht, W., Rahmstorf, S. and Schellnhuber, H., J.~~2008“~~: Tipping elements in the Earth~~?~~'s climate system~~”~~, PNAS 105, 1786–1793~~.~~, 2008.

Lenton, T. M.~~2012“~~: Arctic climate tipping points~~”~~, AMBIO 41, 10–22~~.~~, 2012.

Lewis, G.M. and Langford, W.F.~~2008“~~: Hysteresis in a rotating differentially heated spherical shell of Boussinesq fluid~~”~~, SIAM J. Appl. Dyn. Syst. 7, 1421–1444~~.~~, 2008.

North, G.R., Cahalan, R.F. and Coakley, J.A.~~1981“~~: Energy balance climate models~~”~~, Rev. Geophys. Space Phys. 19, 91–121~~.~~, 1981.

North, G. R. and K.-Y. Kim~~2017~~: Energy Balance Climate Models, Wiley–VCH, Weinheim, Germany~~.~~, 2017.

Nugent, A. D., Smith, R. B., and Minder, J. R.~~2014“~~: Wind speed control of tropical orographic convection~~”~~. J. Atmos. Sci. 71, 2695–2712~~.~~, 2014.

Passchier, S., Bohaty, S. M., Jiménez-Espejo, F., Pross, J., Röhl, U., van de Flierdt, T., Escutia, C. and Brinkhuis, H.: Early Eocene to middle Miocene cooling and aridification of East Antarctica. Geochem. Geophys. Geosys. 14, 1399–1410, 2013.

Payne, A. E., Jansen, M. F. and Cronin, T. W.~~2015“~~: Conceptual model analysis of the influence of temperature feedbacks on polar amplification~~”~~, Geophys. Res. Lett. 42, 9561–9570~~.~~, 2015.

Pierrehumbert, R.T.~~2010~~: Principles of Planetary Climate. Cambridge University Press, Cambridge UK, 2010.

Pistone, K., Eisenman, I. and Ramanathan, V.: Observational determination of albedo decrease caused by vanishing Arctic sea ice. PNAS 111, 3322–3326, 2014.

Pirazzini, R.~~2004“~~: Surface albedo measurements over antarctic sites in summer~~”.~~ , J. Geophys. Res. 109, 2004. D20118.

Proistosescu, C. and Huybers, P. J.~~2017“~~: Slow climate mode reconciles historical and model-based estimates of climate sensitivity~~.”~~, Sci. Adv. 3, 2017. e1602821, DOI: 10.1126/sciadv.1602821.

Sagan, C. and Mullen, G.~~1972“~~: Earth and Mars: Evolution of atmospheres and surface temperatures~~”,~~. Science, New Series 177, 52–56~~.~~, 1972.

Schmidt, G. A., Ruedy, R. A., Miller, R. L. and Lacis, A. A.~~2010. “~~: Attribution of the present day total greenhouse effect~~”~~, J. Geophys. Res. 115, 2010. D20106.

Seager, R. and Battisti, D. S.~~2007“~~: Challenges to our understanding of the general circulation: abrupt climate change~~”~~, In: T. Schneider and Sobel, A.S. (Editors), The Global Circulation of the Atmosphere: Phenomena, Theory, Challenges. Princeton University Press, ~~pp. 331-371.~~ 331–371, 2007.

Sellers, W. D.~~1969“~~: A global climate model based on the energy balance of the Earth–atmosphere system~~”.~~, J. Appl. Meteorol. 8, 392–400~~.~~, 1969.

Serreze, M. C., Barrett, A. P. and Stroeve, J.~~2012“~~: Recent changes in tropospheric water vapor over the Arctic as assessed from radiosondes and atmospheric reanalyses~~”~~, J. Geophys. Res. 117, 2012. D10104, doi:10.1029/2011JD017421.

Shupe, M. D. and Intrieri, J. M.~~2003“~~: Cloud radiative forcing of the ~~arctic~~ Arctic surface: The influence of cloud properties, surface albedo, and solar zenith angle~~”~~, J. ~~Climate~~ Clim. 17, 616–628~~.~~, 2003.

Shupe, M.D., Walden, Von P., Eloranta, E., Uttal, T., Campbell, J. R., Starkweather, S. M. and Shiobara, M.~~2011“~~: Clouds at Arctic atmospheric observatories. Part I: occurrence and macrophysical properties~~”~~, J. Appl. ~~Meteo~~Meteorol. Clim. 50, 626–644~~.~~, 2011.

Steffen, W., Rockström, J., Richardson, K., Lenton, T. M., Folke, C., Liverman, D., Summerhayes, C. P., Barnosky, A. D., Cornell, S. E., Crucifix, M., Donges, J. F., Fetzer, I., Lade, S. J., Scheffer, M., Winkelmann, R. and Schellnhuber, H. J.~~2018“~~: Trajectories of the Earth system in the Anthropocene~~”, PNAS~~ , PNAS 2018. www.pnas.org/cgi/doi/10.1073/pnas.1810141115.

Stranne, C., Jakobsson, M. and Björk, G.~~2014“~~: Arctic Ocean perennial sea ice breakdown during the Early Holocene Insolation Maximum~~”~~, Quart. Sci. Rev. 92, 123–132~~.~~, 2014.

Thorndike, A.~~2012“~~: Multiple equilibria in a minimal climate model~~”~~, Cold Reg. Sci. Technol., 76, 3–7, 2012. https://doi.org/10.1016/j.coldregions.2011.03.002.

Trenberth, K. E., Fasullo, J. T., and Kiehl, J.~~2009“~~: Earth's global energy budget~~”~~, B. Am. Meteorol. Soc. 90, 311–323~~.~~, 2009.

Valdes, P.~~2011“~~: Built for stability~~”~~, Nature Geosci. 4, 414–416~~.~~, 2011.

van Vuuren, D. P., Edmonds, J., Kainuma,M., Riahi, K., Thomson, A., Hibbard, K., Hurtt, G. C., Kram, T., Krey, V., Lamarque, J.-F., Masui, T., Meinshausen, M., Nakicenovic, N., Smith, S. J. and Steven K. Rose, S. K.: The representative concentration pathways: an overview, Clim. Change 109, 5–31, 2011.

Wallace-Wells, D.~~2019~~: The Uninhabitable Earth: Life After Warming. Penguin Random House LLC, New York~~.~~, 2019.

Wild, M., Folini, D., Schär, C., Loeb, N., Dutton, E. G. and König-Langlo, G.~~2013“~~: The global energy balance from a surface perspective~~”. Climate Dynamics~~ , Clim. Dyn. 40, 3107–3134~~.~~, 2013.

Willard, D. A., Donders, T. H., Reichgelt, T., Greenwood, D. R., Sangiorgi, F., Peterse, F., Nierop, K. G. J., Frieling, J., Schouten, S. and Sluijs, A.: Arctic vegetation, temperature, and hydrology during Early Eocene transient global warming events, Global and Planetary Change 178, 139–152, 2019.

Wu, X., Budd, W. F., Worby, A. P. and Allison, I. ~~2001“~~Sensitivity of the Antarctic sea-ice distribution to oceanic heat flux in a coupled atmosphere-sea-ice model~~”~~, Ann. ~~Glaciology~~ Glaciol. 33, 577–584~~.~~, 2001.

Yang, H., Zhao, Y.-Y. and Liu, Z.-Y.~~2016“~~: Understanding Bjerknes compensation in atmosphere and ocean transports using a coupled box model~~”~~, J. ~~Climate~~ Clim. 29, 2145–2160~~.~~, 2016.

Zeebe, R. E.~~2011“~~: Where are you heading Earth? ~~”,~~Nature Geosci. 4, 416–417~~.~~, 2011.

Zhang, Y.-C. and Rossow, W. B.~~1997“~~: Estimating meridional energy transports by the atmospheric and oceanic circulations using boundary fluxes~~”~~, J. ~~Climate~~ Clim. 10, 2358–2373~~.~~, 1997.

Table 1. Summary of variables and parameters used in the EBM. The values of the physical constants $\xi_a, \xi_R, k_C, k_W, G_C, G_{W1}, G_{W2}$ are as determined in Kypke (2019); Dortmans et al. (2019).

Variables	**Symbol**	**Value**
Mean temperature of the surface	T_S	-50 to + 40 C
Infrared radiation from the surface	$I_S = \sigma T_S^4$	141 to 419 W m^{-2}
Mean temperature of the atmosphere	T_A	-70 to + 10 C
Energy emitted by the atmosphere	$I_A = \epsilon \sigma T_A^4$	87 to 219 W m^{-2}
Parameters and Constants	**Symbol**	**Value**
Temperature of freezing point for water	T_R	273.15 K
Stefan–Boltzmann constant	σ	5.67×10^{-8} W m^{-2} K^{-4}
Emissivity of dry air	ϵ	0.9
Greenhouse gas absorptivity	η	0 to 1
Absorptivity for CO_2	η_C	0 to 1
Absorptivity for H_2O	η_W	0 to 1
Absorptivity for clouds	η_{Cl}	0.255
Portion of I_A reaching surface	β	0.63
Ocean heat transport	F_O	10 W m^{-2}
Atmospheric heat transport	F_A	104 W m^{-2}
Vertical heat conduction and latent heat	F_C	20 to 120 W m^{-2}
Absorption of solar radiation	F_S	$(1-\alpha)Q$
Incident solar radiation at Poles	Q_P	173.2 W m^{-2}
Incident solar radiation at Equator	Q_E	418.8 W m^{-2}
Fraction of insolation absorbed by atmosphere	ξ_A	0.2324
Fraction of insolation reflected by clouds	ξ_R	0.1212 (poles) 0.2235 (global)
Molar concentration of CO_2 in ppm	μ	270 to 2000 ppm
Relative humidity of H_2O	δ	0 to 1
Absorption coefficient for CO_2	k_C	0.07424 m^2 kg^{-1}
Absorption coefficient for H_2O	k_W	0.05905 m^2 kg^{-1}
Warm surface albedo for ocean	α_w	0.08
Cold surface albedo for Arctic	α_c	0.7
Albedo transition rate (in tanh function)	$\omega = \Omega / T_R$	0.01
ICAO standard atmosphere lapse rate	Γ	6.49×10^{-3} K m^{-1}
Normalized standard lapse rate	$\gamma = \Gamma / T_R$	2.38×10^{-5} m^{-1}
Tropopause height at North Pole	Z_P	9000 m
Latent heat of vaporization of water	L_v	2.2558×10^6 m^2 s^{-2}
Universal ideal gas constant	R	8.3145 kg m^2 s^{-2} K^{-1} mol^{-1}
Ideal gas constant specific to water vapour	R_W	461.4 m^2 s^{-2} K^{-1}
Saturated partial pressure of water at T_R	$P_W^{sat}(T_R)$	611.2 Pa

Table 2. Atmosphere and ocean heat fluxes into the Arctic as simulated in Koenigk and Brodeau (2014), using the global coupled climate model EC-Earth.

Year	Scenario	F_A (W/m^2)	F_O (W/m^2)
1850	Historical	107.28	9.75
2100	RCP 2.6	104.03	13.00
2100	RCP 8.5	97.53	19.50

~~Atmosphere and ocean heat fluxes into the Arctic as simulated in (Koenigk and Brodeau (2014)), using the global coupled climate model EC-Earth.~~

Table 3. ECS for the globally averaged EBM.

	τ_S	°C
$\mu = 270$	~~1.0542~~1.0561	~~14.812~~ 15.324
$\mu = 540$	~~1.0709~~ 1.0720	~~19.363~~19.667
ECS	~~0.016663~~0.0047	~~4.5516~~ 4.343

~~ECS (in °C) for the globally averaged EBM.~~

Table 4. ECS values for each of the three regional EBMs. The ECS is much greater for the Poles than for the Tropics, in agreement with observations.

Arctic Region

	τ_S	°C
$\mu = 270$	~~0.8853~~ 0.8829	~~-31.34~~ -31.981
$\mu = 540$	~~0.9145~~ 0.9120	~~-23.34~~ -24.027
ECS	0.0293	~~7.995~~ 7.9535

Antarctic Region

	τ_S	°C
$\mu = 270$	~~0.8671~~ 0.8693	~~-36.30~~ -35.691
$\mu = 540$	~~0.8947~~ 0.8970	~~-28.77~~ -28.147
ECS	0.0276	~~7.531~~ 7.5434

Tropic Region

	τ_S	°C
$\mu = 270$	~~1.091~~1.0890	~~24.74~~24.319
$\mu = 540$	~~1.095~~ 1.0937	~~25.87~~25.592
ECS	~~0.0041~~ 0.0047	~~1.128~~ 1.2727

~~ECS values (in °C) for each of the three regional EBMs. The ECS is much greater for the Poles than for the Tropics, in agreement with observations.~~